ERDC/CHL CR-10-4

US Army Corps
of Engineers®
Engineer Research and
Development Center

Urban Flood Damage Reduction and Channel Restoration Development and Demonstration Program for Arid and Semi-Arid Regions (UFDP); Southwest Urban Flood Damage Program (SWDP)

Evapotranspiration, Water Table Fluctuations, and Riparian Restoration: Report Documentary 2007-2008 Work

James R. Cleverly, Kristin Vanderbilt, Cliff Dahm,
James R. Thibault, and Maceo Carrillo Martinet

September 2010

Coastal and Hydraulics Laboratory

Urban Flood Damage Reduction and Channel Restoration Development and Demonstration Program for Arid and Semi-Arid Regions (UFDP); Southwest Urban Flood Damage Program (SWDP)

ERDC/CHL CR-10-4
September 2010

Evapotranspiration, Water Table Fluctuations, and Riparian Restoration: Report Documentary 2007-2008 Work

James R. Cleverly, Kristin Vanderbilt, Cliff Dahm, James R. Thibault, and Maceo Carrillo Martinet

University of New Mexico
MSC01 1070 Civil Engineering
Albuquerque, NM 87120

Final report

Prepared for U.S. Army Corps of Engineers
Washington, DC 20314-1000

Monitored by Coastal and Hydraulics Laboratory
U.S. Army Engineer Research and Development Center
3909 Halls Ferry Road, Vicksburg, MS 39180-6199

Abstract: Water use by riverside phreatophyte ecosystems, also referred to as evapotranspiration or just ET, makes up a significant proportion of a river basin's water budget depletions. As phreatophytes, riparian plants access groundwater for their water supply. The objective of this study is to characterize ET depletions from various representative riparian land cover types and to describe the groundwater-vegetation interactions that relate ET to local hydrology. Measurements of ET and groundwater are made at various locations within the city of Albuquerque, NM, and along the Middle Rio Grande. ET is measured from eddy covariance flux towers and groundwater levels are continuously monitored using commercially available submersible pressure transducers. Results show that modest water salvage can be claimed from riparian restoration projects that are properly implemented while additional water losses are possible when necessary follow-up is not undertaken. Bare soil is shown to lose less water to evaporation than previously expected, and urban hydrology (e.g., waste water return) maintains high ET rates in whichever species grow in the outfall. Remote sensing of riparian vegetation clearly shows the effects of fires in the urban reach, the initial decline in vegetation density, leaf area index, and ET. This research illustrates the importance of identifying the hydrologic and vegetative factors controlling ET in a large, urban river system.

Contents

Figures

Figures

Preface

The research presented in this report was developed by the University of New Mexico (UNM) under the direction of the U.S. Army Engineer Research and Development Center (ERDC), Coastal and Hydraulics Laboratory (CHL), Technical Programs Office. Funding was provided by the Urban Flood Damage Reduction and Channel Restoration Development and Demonstration Program for Arid and Semi-Arid Regions (UFDP) and Southwest Urban Flood Damage Program (SWDP) of the USACE General Investigation Research and Development Program. Authorization of the U.S. Army Corps of Engineers to conduct research and development is codified in 10 U.S.C. 2358.

Work was performed under the general supervision of Dr. Lisa C. Hubbard, UFDP and SWDP Program Manager, Dr. Jack E. Davis, Technical Director for Flood and Coastal Storm Damage Reduction, William R. Curtis, Program Manager of the Flood and Coastal Storm Damage Reduction Research and Development Program, Dr. William D. Martin, Director, CHL, and Jose Sanchez, Deputy Director, CHL. This report was prepared by Dr. Tim F. Wawrzyniec, Jed D. Frechette, Dr. Julie Coonrod, and Dr. John Stormont, all of the University of New Mexico. Technical reviews was conducted by Ondrea Hummel of the U.S. Army Engineer District, Albuquerque, and Dr. Hubbard.

COL Gary E. Johnston was Commander and Executive Director of ERDC. Dr. Jeffery P. Holland was Director of ERDC.

1 Introduction

Restoration efforts that remove non-native understory vegetation or dense monotypic stands of non-native vegetation from riparian zones (the bosque) are designed to reduce consumption of water. Quantification of the response of evapotranspiration (ET) and water table depths to non-native understory removal or to eradication of dense stands of non-native species like salt cedar (*Tamarix chinensis*) or Russian olive (*Elaeagnus angustifolia*) is needed to provide defensible estimates of potential water-savings from restoration activities. In addition to restoration assessment, it is also important to monitor the increasing roles of fire and post-fire management on ET and water tables. The ET and water table responses of a site with understory removed (Albuquerque South Valley) was monitored. In addition, an investigation was conducted on how a wildfire in June 2006 has affected evaporative rates and water table fluctuations at the Albuquerque site, which is in close proximity to the Rio Grande. Scaling the information on ET at various sites along the Albuquerque reach of the Rio Grande will require the use of remote sensing methodology. Using 2006 multispectral imagery, an update was made of a 2002 vegetation classification that was developed for the middle Rio Grande to show where major changes in vegetation due to fire or mechanical removal have occurred in the last 4 years (Figure 1). This report: (1) highlights and reports ET data using eddy covariance technology, (2) documents water table dynamics and fluctuations at the ET site, (3) presents remote sensing results comparing vegetation type and normalized difference vegetation index (NDVI), and (4) presents initial results from the groundwater flow field study, which evaluates changes in water table elevation with changing river discharge.

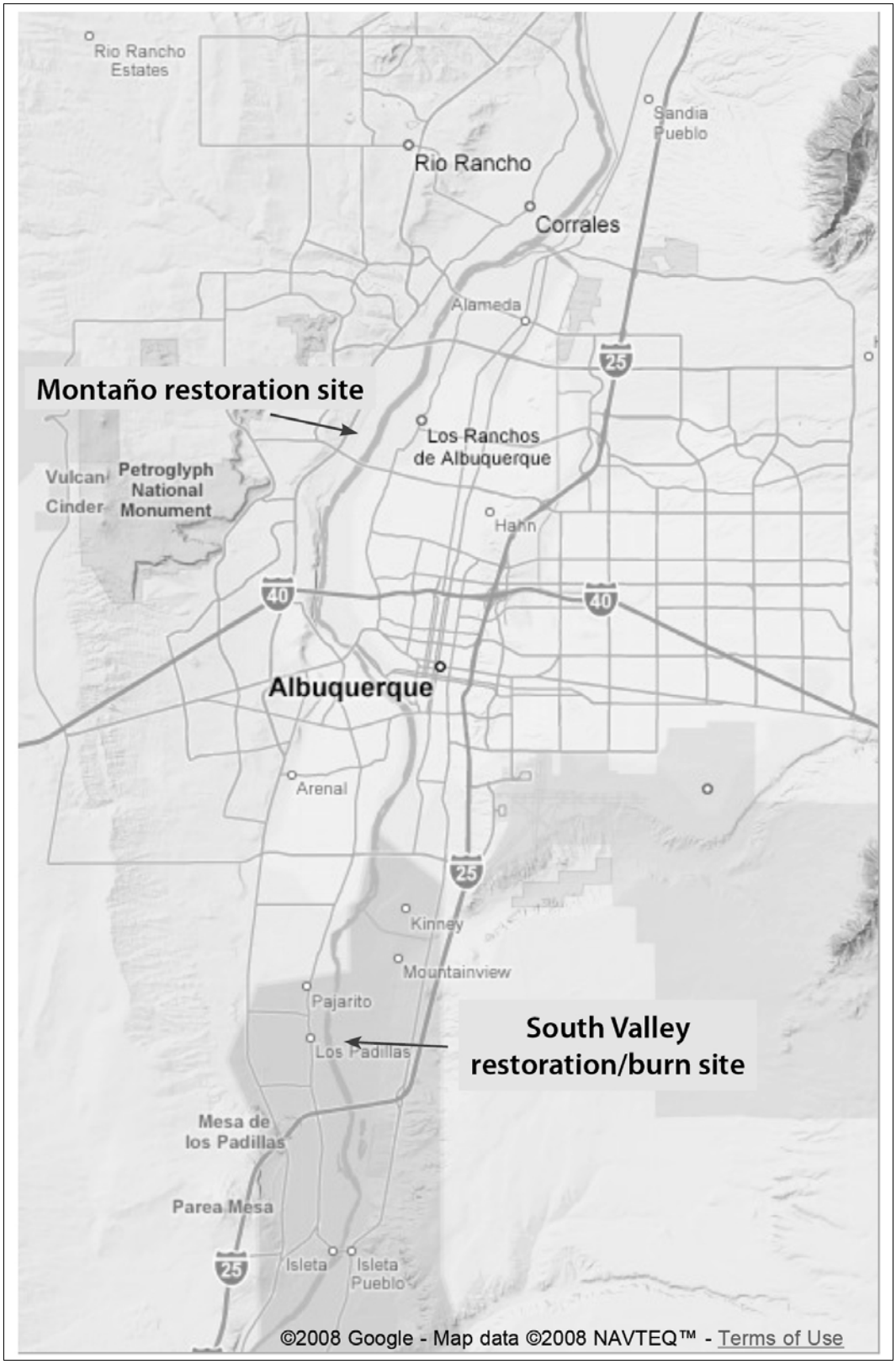

Figure 1. Map of restoration and burn sites in urban reach of Albuquerque, NM.

2 Evapotranspiration (ET)

Overview

Evapotranspiration (ET) is a major component of the water budget of both aquatic and terrestrial ecosystems. Dahm et al. (2002) showed that the riparian zone (bosque) of the Rio Grande from the U.S. Geological Survey (USGS) Otowi gage to the outlet of Elephant Butte Reservoir accounts for one-quarter to one-third of the depletions along this reach of river. Accurate characterization of the rates of ET from riparian vegetation and the factors that control these rates are needed. The Urban Flood Damage Reduction and Channel Restoration Development and Demonstration Program for Arid and Semi-Arid Regions (UFDP) and Southwest Urban Flood Damage Program (SWDP) have allowed the continued measurement of riparian zone ET from a cottonwood site in the South Valley of Albuquerque. The site had the non-native vegetation in the understory removed in the winter of 2004, and the initial research plan was to evaluate the water use in this bosque with non-native plants mechanically removed. A human-caused fire on 15 June 2006 burned the vegetation on the south side of the tower where ET rates are measured. Therefore, the summer of 2006 became an opportunity to address the effect of fire on ET rates in a cottonwood forest along the Rio Grande, and the chance to consider another factor affecting ET rates in the bosque of the Rio Grande (Cleverly et al. 2002; Shafroth et al. 2005; Cleverly et al. 2006).

Methodology

Three-dimensional (3-D) sonic eddy covariance (3SEC) is the benchmark method for measuring fluxes over tall vegetation, under advection, and in complex terrain (Brunet et al. 1994; McAneney et al. 1994; Simpson et al. 1998; Drexler et al. 2004). One advantage of the 3SEC system is that ET is measured directly, rather than estimated as the residual of the energy balance (Equation 1). Thus, 3SEC is the only method that provides the means of estimating energy balance closure error as a self-check for accuracy (Twine et al. 2000; Drexler et al. 2004).

The core instruments in 3SEC systems are a 3-D sonic anemometer to measure wind speed in three dimensions, a krypton hygrometer or an infrared gas analyzer (IRGA) to measure humidity, a thermocouple with a

fine-wire junction (0.0127 mm diam type E chromel–constantan) to avoid signal retention in high frequency measurements. Each of these instruments make measurements at a frequency determined through spectral decomposition of sample time series taken at 20 Hz. A sampling frequency is chosen in the high-frequency spectral gap, usually between 5 and 20 Hz (Stull 1988).

Latent heat flux (λE), or the heat absorbed by evaporation, is computed from these measurements as a function of the covariance between vertical wind speed and humidity:

$$\lambda E = \lambda \overline{w'q'} = \lambda \sum_{i=1}^{n} \frac{(w_i - \bar{w})(q_i - \bar{q})}{n} = \lambda \mathrm{Cov}(wq) = \lambda \rho_w \mathrm{ET} \qquad (1)$$

where λ is the latent heat of vaporization, w' is the instantaneous deviation from mean vertical wind speed (i.e., $w' = w_i - \bar{w}$), and q' is the instantaneous deviation from average water vapor density. The time period for averaging, n, is chosen from balancing the spectral gap with minimizing trending in low frequencies. Covariance periods are typically 15 to 40 min long. Sensible heat flux (H, heat transfer due to vertical atmospheric temperature gradients) is computed likewise as a function of the covariance between vertical wind speed and temperature:

$$H = C_p \rho_a \overline{w'T'} = C_p \rho_a \sum_{i=1}^{n} \frac{(w_i - \bar{w})(T_i - \bar{T})}{n} = C_p \rho_a \mathrm{Cov}(wT) \qquad (2)$$

where ρ_a is density of wet air, and T' is the instantaneous deviation of temperature from mean air temperature.

Before ET is computed from λE, various standard corrections are applied to incorporate the physical realities within which these measurements are made. These corrections include coordinate rotation to align the wind vector with the sonic anemometer (Wesely 1970), corrections developed from frequency response relationships which incorporate sensor line averaging and separation (Massman 2000, 2001), correction to account for flux effects on vapor density measurements as opposed to mixing ratio measurements (Webb et al. 1980), and krypton hygrometer oxygen and second-order humidity effects on vapor density measurements. Lastly, closure of the energy balance is forced into thermodynamic equilibrium by

adding closure energy into H and λE in relation to the measured Bowen ratio (Twine et al. 2000; Cleverly et al. 2002).

Measurement of turbulent fluxes via 3SEC involves measuring flux variables from a tower or an aircraft. When measurements are made from a tower, the minimum spacing between a canopy and the sensors is dictated by the necessity to make measurements above the roughness sublayer. The top of the roughness sublayer is equal to the distance of the aerodynamic roughness length, z_0, above the canopy, h_c (Nakamura and Mahrt 2001). The upper limit for sensor placement in riparian corridors is chosen to remain below the top of the surface layer and to minimize the measurement footprint (Cooper et al. 2000; Cooper et al. 2003). The top of the surface layer is defined in terms of Monin-Obukhov (M-O) similarity theory, which describes the physics of the atmospheric surface layer (Stull 1988). Atmospheric stability imposed by advection is associated with vertical thermal stratification and compression of the surface layer to the lower few meters above the canopy (Cooper et al. 2003).

The planetary boundary layer is that lower portion of the atmosphere where turbulence dominates vertical transport and friction creates a strong drag on near-surface winds. The surface layer makes up the bottom 10 percent of the boundary layer (Stull 1988), where surface drag creates a near-logarithmic wind speed profile. The vertical gradient in horizontal wind speed causes deformation of the air column and generates turbulence that can be characterized by Reynolds stress, τ_{Reynolds}, which is equal to the total vertical flux of horizontal momentum in the surface layer (Stull 1988):

$$\left|\tau_{\text{Reynolds}}\right| = \overline{\rho}\left[\left(\overline{u'w'}\right)^2 + \left(\overline{v'w'}\right)^2\right]^{1/2} \tag{3}$$

where ρ is density of air, and u, v, and w are orthogonal wind speeds in two horizontal and one vertical dimensions, respectively. The velocity scale across which Reynolds stresses are propagated is the friction coefficient, u_* (Stull 1988):

$$u_* = \frac{\left|\tau_{\text{Reynolds}}\right|}{\rho} = \left[\left(\overline{u'w'}\right)^2 + \left(\overline{v'w'}\right)^2\right]^{1/2} \tag{4}$$

The friction coefficient is important in describing the magnitude of turbulence in the surface layer, and that prominence is central to the body

of the relationships known as M-O similarity theory. M-O similarity theory, also known as surface layer similarity theory, is a body of empirical relationships that characterize turbulence in the surface layer. Other M-O scales useful for characterizing the surface layer include the humidity scale, q_*, the temperature scale, θ_*, and the Obukhov length, L (Stull 1988):

$$q_* = \frac{-\overline{w'q'}}{u_*}, \tag{5}$$

$$\theta_* = \frac{-\overline{w'T'}}{u_*}. \tag{6}$$

$$L = \frac{-\bar{T}u_*^2}{kg\theta_*} \tag{7}$$

where k is von Kármán's constant and g is the acceleration due gravity. When L is zero, the surface layer is neutrally stratified. When negative, the surface layer is unstably stratified, and the temperature profile in the surface layer is stable when L is positive. The Semi-Arid Land-Surface-Atmosphere (SALSA) program, which brought together eddy covariance and Lidar (light detection and ranging) technologies to measure ET in the San Pedro River of Arizona, generated the first detailed characterization of the turbulent boundary layer in a riparian corridor (Cooper et al. 2000; Goodrich et al. 2000; Kao et al. 2000; Scott et al. 2000).

The measurement footprint represents the upwind distance that is incorporated into measurements made by instruments on the tower. The footprint increases with height above the canopy and with wind speed (Rannik et al. 2000). In riparian forests along the Middle Rio Grande and the San Pedro River, the footprint for sensors mounted 2.5 m above Tamarix may be as little as 40 to 60 m under ideal conditions or up to 200 m over *Populus fremontii* (Fremont cottonwood).

Results

An aerial view of the South Valley site where ET measurements are made is shown in Figure 2. The ET tower is located in the broader swath of bosque in the foreground of the figure. Restoration of the forest, performed by mechanical removal of understory vegetation, was begun during the winter of 2002-2003, of which only the nearest 30 m of the tower's footprint was

affected. Completion of the restoration project was achieved before the 2004 growing season. The fire on 15 June 2006 effectively burned the vegetation to the south of the tower. In fact, the road to the tower site became the fire break used to contain the fire. Soil temperatures exceeded 100°C at 10-cm depth during the fire and soil heat flux values reached almost 500 W/m^2. Some of the instruments on the tower were damaged by the fire. Damaged instruments were repaired and replaced as soon as access was granted and new instruments could be procured. The site was back on-line and measuring ET beginning 18 July 2006.

Figure 3 illustrates the Palmer Drought Severity Index (PDSI) and estimated snowpack conditions for the period of record. Since January 2000, the Upper and Middle Rio Grande has experienced prolonged extreme drought (2001-2004) interspersed with shorter periods of normal or moderately wet conditions.

Figure 4 shows the measured ET rates at the Albuquerque South Valley site for the period of record. Early growing season values for ET ramped up quickly in the late spring after leaf out. Maximum rates near 9 or 10 mm/day were common, especially on days in late May and early June. These values approach the theoretical maximum rate of ET for a clear sunny day at this time of year. The high ET rates indicate a high rate of primary production from the riparian forest during this period.

In 2006, ET rates were generally much lower after the fire, when the equipment was replaced and measurements began on 18 July. Occasional higher rates were observed due to a stronger contribution from the unburned forest north of the tower. Average values ramped downward from < 7 mm/day in late July to around 4 mm/day in mid-September. Senescence occurred in September and October with ET rates falling to background levels by late October after the first hard freezes. The growing season of 2006 represents the seventh year of ET measurements at this site.

In 2004, a precipitous decline in ET coincided with restoration follow-up activities in which contractors returned to the site, mechanically removed resprouting vegetation, and applied an herbicide to freshly-cut stems. In post-restoration years, ET rates were lower if and only if understory revegetation was curtailed, either through restoration activities or due to fire (Figure 5). Xeroriparian areas inhabited by saltcedar, saltgrass, and

saltbush have consistently lower ET rates than wetter sites containing obligate riparian species. Dense, monospecific saltcedar thickets have the highest ET rates, followed by mixed cottonwood and non-native forests, young Russian olive and willow thickets, and then native cottonwood forests, which have lower ET rates than the other mesic riparian species.

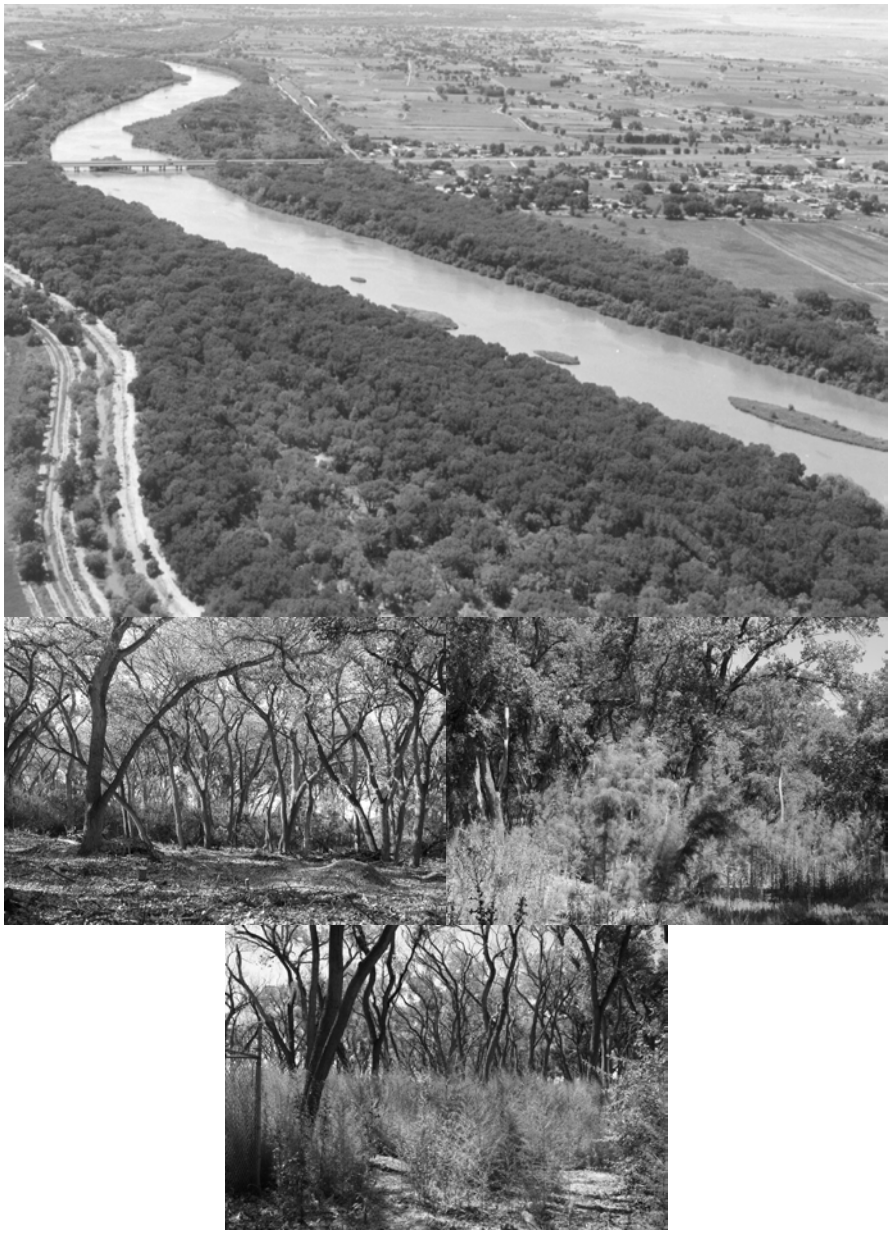

Figure 2. Top photograph is aerial view of South Valley of Albuquerque ET measurement site looking south. Tower is located in wider portion of bosque in foreground. Bridge in background is the Interstate 25 bridge over Rio Grande near Isleta. This photograph was taken in early summer of 2000 before Maplais Fire (June 2006). Lower photographs, clockwise from upper left: Partially-cleared understory, 21 November 2002; vegetative propagation of previously-cleared saltcedar, 26 July 2007; riparian annual weeds growing on sunlit soil, 26 July 2007.

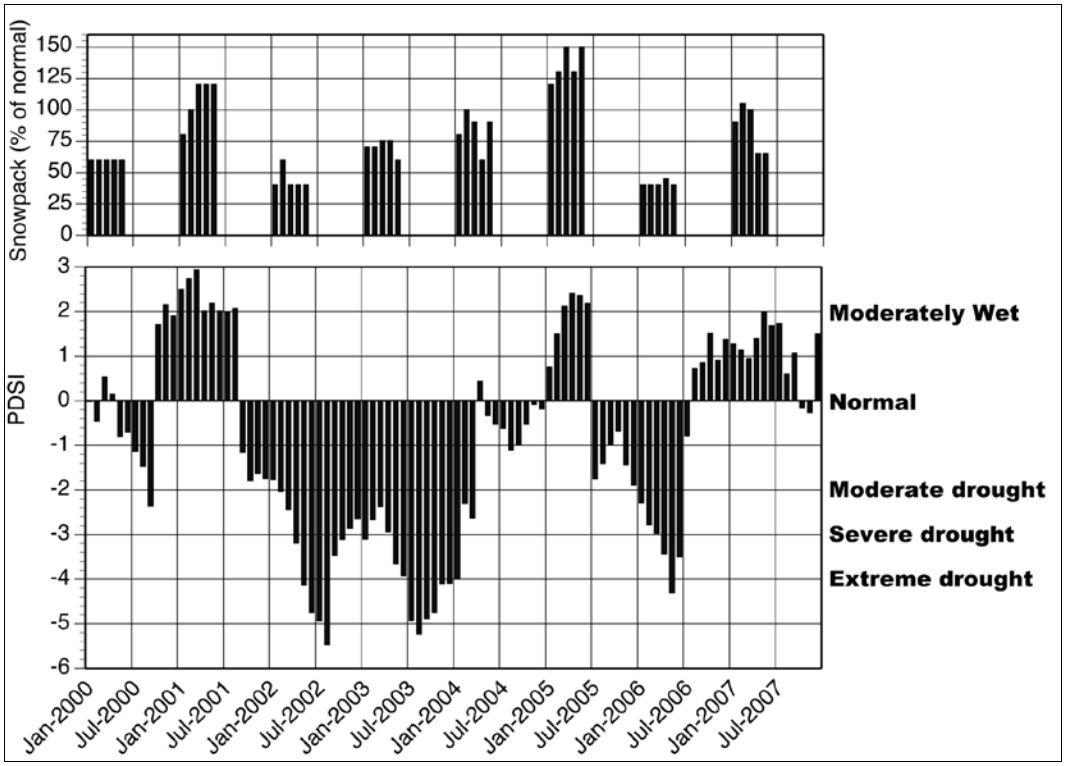

Figure 3. Monthly average snowpack and PDSI. Values represent average of New Mexico Region 2 (Upper Rio Grande) and Region 5 (Middle Rio Grande), and Colorado Region 5 (Rio Grande headwaters).

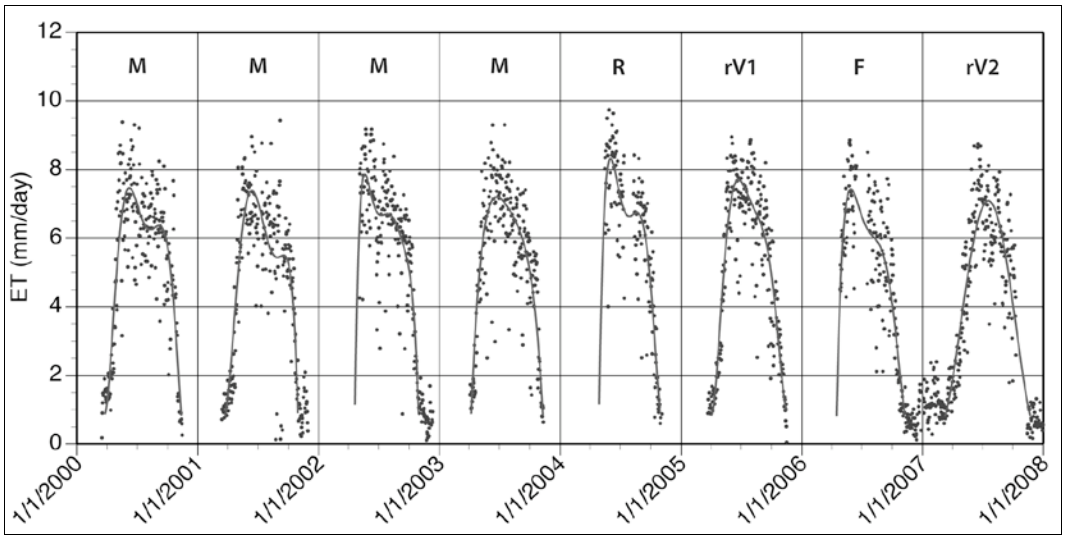

Figure 4. Rates of evapotranspiration (ET) at Albuquerque South Valley tower site for period of record. Lines represent polynomial least squares regression. Forest community is described as mixed cottonwood, saltcedar and Russian olive (M; 2000-2003), restored monospecific cottonwood forest (R; 2004), cottonwood with self revegetating saltcedar and Russian olive (rV1; 2005), burned cottonwood forest (F, June 2006), and cottonwood forest with monsoon-season annuals in open, sunlit spaces (rV2; 2007).

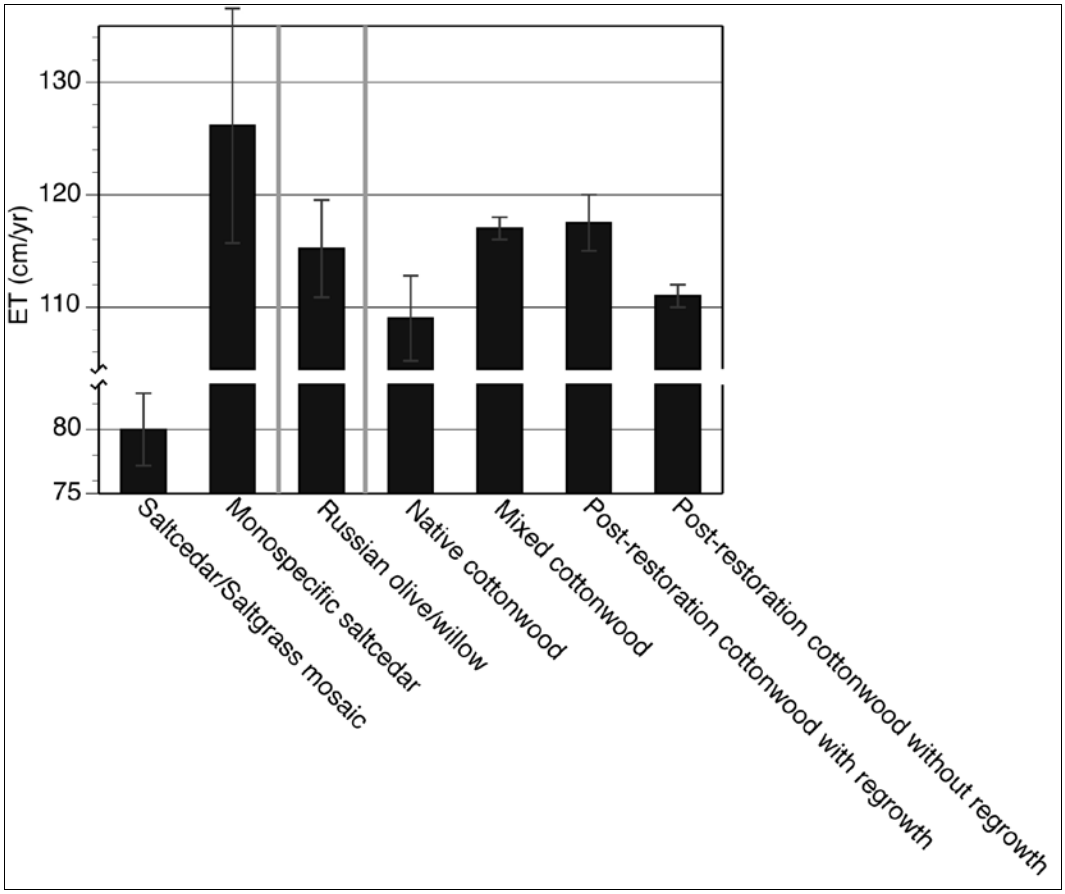

Figure 5. Total accumulated ET during growing season for indicated forest community types.

Figure 6 shows that cottonwood forest ET responds to summer drought but not to winter drought and snowpack conditions. During summer months, monsoon activity is characterized by lower net radiation and vapor pressure deficit, both contributing factors to reduced ET. Three of the four post-restoration years have positive residuals, indicating that summer ET was higher than expected for the given drought conditions when new-growth understory is present.

The bare soil site on the Rio Salado was in operation for approximately 100 days before a catastrophic flood destroyed and scatted the system. A new system was built at Bosque del Apache at the National Wildlife Refuge (NWR) to monitor bare soil fluxes outside of the active channel. Figure 7 shows the locations of these sites. Figure 8 verified that precipitation alone accounts for ET from bare surfaces at both sites during the spring and early summer. Figure 8 also shows that, while the ET precipitation (PPT) ratio is 1:1 for bare soil, *Kochia* colonizes the site in early July and the ET:PPT ratio climbs to 2.5:1. In comparison, phreatophytes support ET:PPT ratios of 5:1 and higher.

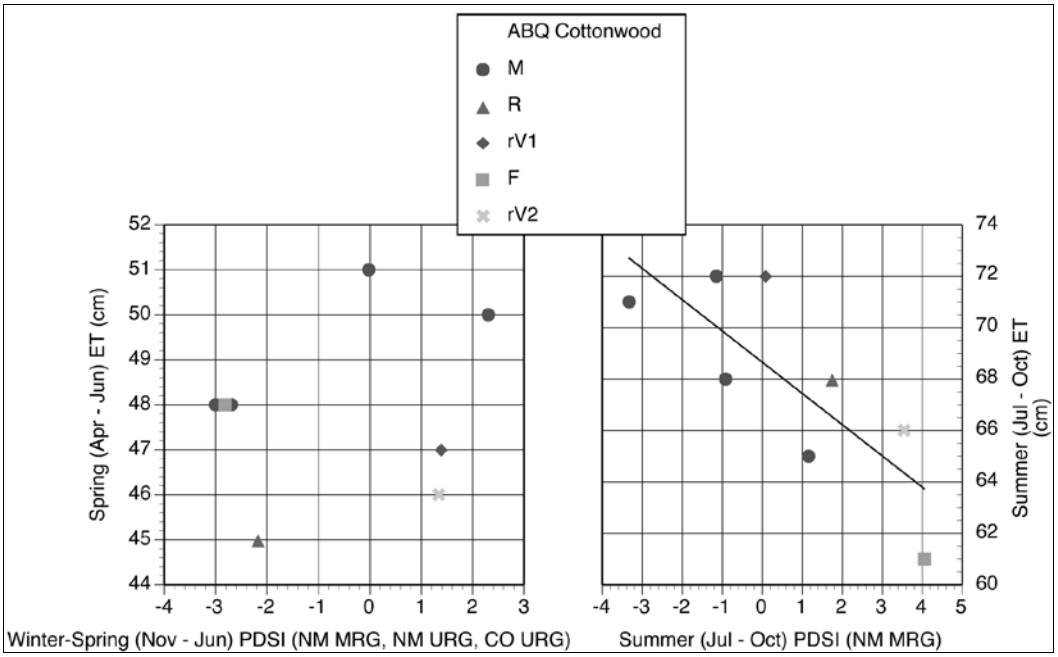

Figure 6. Spring and summer intraseasonal ET with respect to PDSI. Groupings by year are defined in Figure 4.

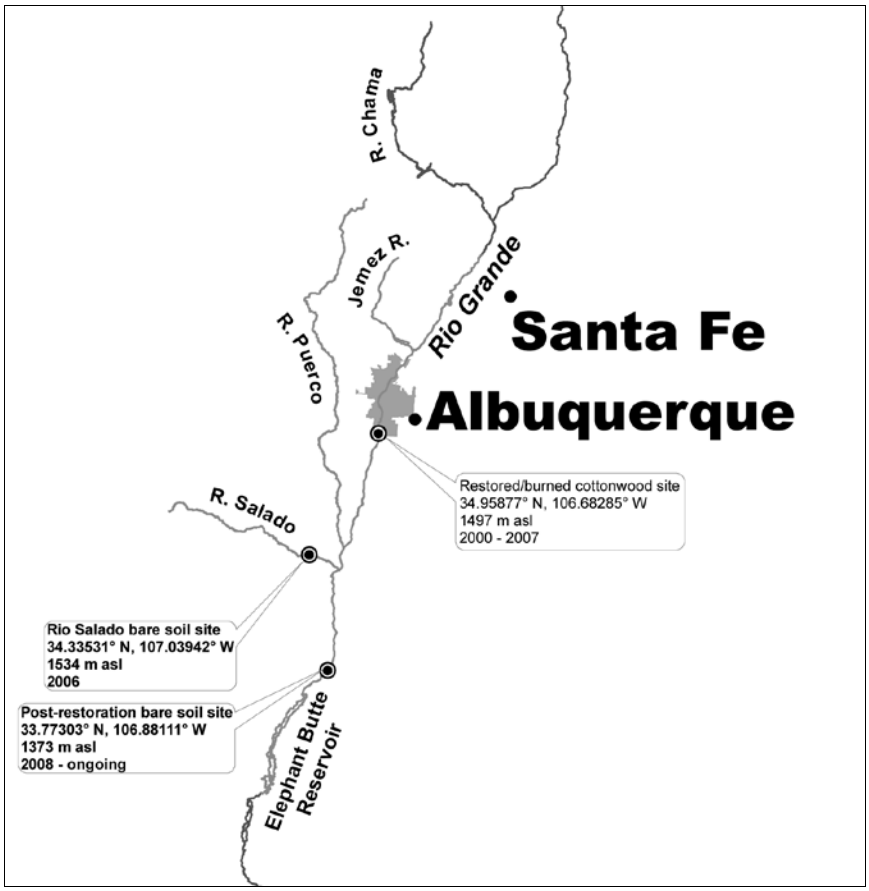

Figure 7. Locations of bare soil sites.

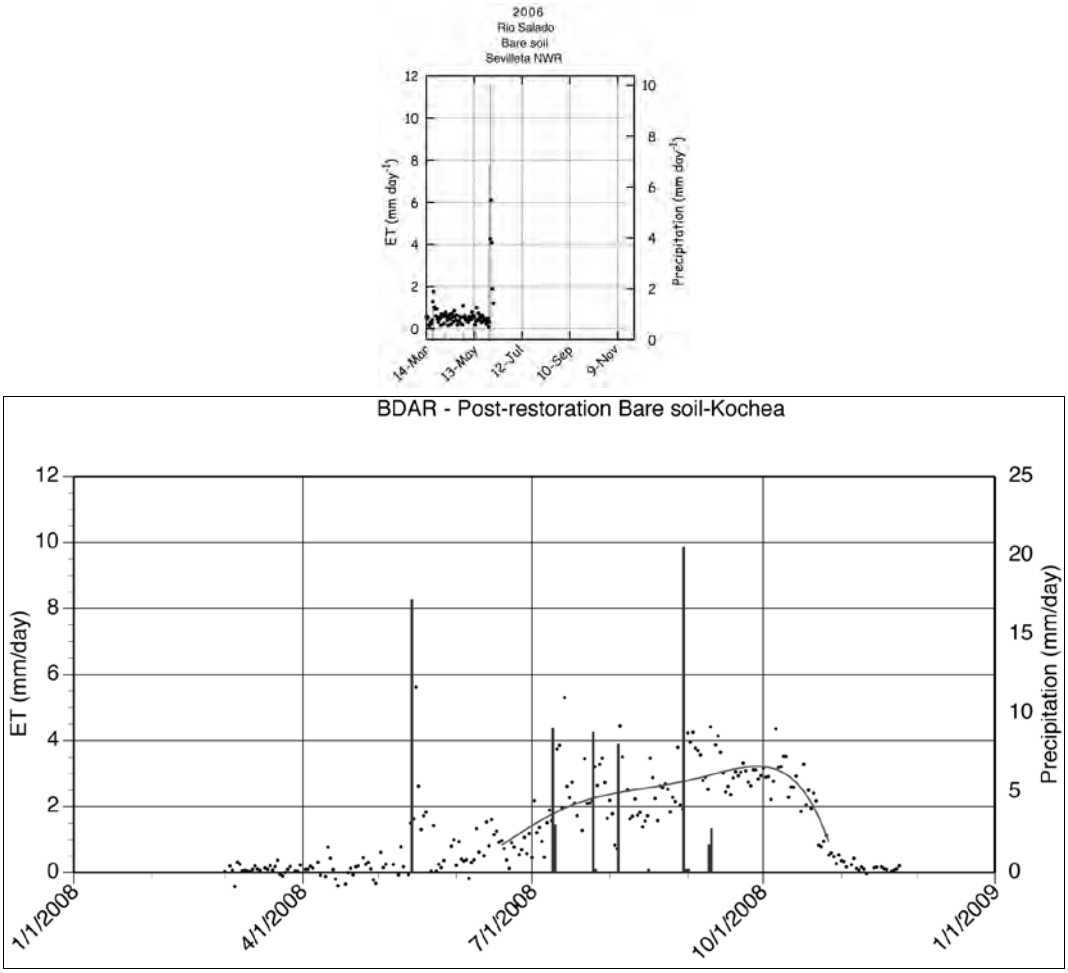

Figure 8. ET and PPT measured at bare soil sites, Rio Salado (top panel) and Bosque del Apache post-restoration (bottom panel). *Kochia* colonized the post-restoration site during late June/early July.

3 Water Table Dynamics

Overview

The water table in the riparian zone provides a measure of the connectivity between the surface water of the Rio Grande and the shallow alluvial groundwater. In addition, the ET activity of the riparian vegetation impacts the level of the water table by extraction of groundwater and transferring this water to the atmosphere through plant transpiration. The interaction between the water table of the shallow alluvial groundwater and the transpiring plants can be seen in both a seasonal signal during the growing season and a daily pattern between water levels during the day and the night. Co-locating groundwater wells with pressure transducers and data loggers at a site with a 3-D eddy covariance flux measurement system for determining ET allows the analysis of the interactions between the shallow alluvial groundwater and the flux of water to the atmosphere.

Methodology

Five shallow groundwater monitoring wells exist at the site. The wells are constructed of 5.1-cm internal diam Schedule 40 PVC pipe installed in 7.6-cm diam manually augured bore holes, to depths approximately 100 cm below the base flow water table. The lower section of each well, approximately 100 cm, consists of a 0.25-mm slotted screen intake. Silica sand and bentonite were used for the filter packs and surface seal, respectively.

As of 2008, four wells include automated sensors logging water level and temperature data every 30 min. Three of the wells are equipped with 3001 M10 Mini LT Leveloggers (Solinst, ON, Canada). At the center well, a DI241 Diver (Waterloo Hydrogeologic, ON, Canada) replaced a Solinst logger on 27 June 2006 that was destroyed by the wildfire 12 days earlier. These pressure transducers have a head range of 9 to 10 m and a resolution of 2 to 3 mm. They measure the absolute pressure (water pressure plus atmospheric pressure) of the water column. To compensate for this, a Solinst Barologger is deployed at the site, which quantifies the atmospheric pressure in water column equivalents. These values are subtracted from the well logger outputs to arrive at actual head levels.

All raw data files from the well loggers are calibrated to manual head measurements taken with a sounding water level meter when data are collected. Sensor data are corrected to manual measurement data using an average offset value or with programs (e.g., FORTRAN, SAS) that compute corrected values in the time series using a linearly varying equation. The processed files are then imported into Excel and SigmaPlot software, where depth to water table values are calculated from the head values and graphed.

Groundwater wells were added to the Montaño restoration site, where monitoring is ongoing and initial results have not yet been reported.

Results

Water table depths below the ground surface from late April through December of 2006 are shown on Figure 9. The first half of 2006 was exceptionally dry with a weak spring snowmelt throughout the Rio Grande basin. Depth to the water table was about 1.8 m with only a weak upward response in late May and June. The monsoons of 2006, however, were unusually strong beginning in late June. Numerous decreases in water table depth (rising groundwater) occurred during river spates from the strong thunderstorm-produced floods from late June to early September with water table depths reaching about 1.4 m below the ground surface. Early fall was a period of dropping water tables until the end of the irrigation season in October when the water table rebounded as less water was diverted to the ditches for irrigation and more flow remained in the river.

A long-term record of water table depths is available for this site (Figure 10). Water table measurements began in the spring of 1999. The long-term record shows the responsiveness of the site to discharge in the Rio Grande. Snowmelt peak flows in the river in 1999, 2001, 2004, and 2005 are clearly seen in the rising water table depth at the Albuquerque South Valley site. The highest water table at the site occurred in May and June of 2005 when peak flows in the Rio Grande reached about 6500 cu ft/sec. The bosque at this site is disconnected from the river and overbank flooding has not occurred at the site since the completion of Cochiti Reservoir in 1975. The unusually strong summer monsoon in 2006 is seen in both river discharge (Q) and the strong water table fluctuations in the summer of 2006. The strong drought years of 2002 and 2003 also seen in the long-term record with maximum water table depth at the site occurring in the late summer of 2003.

Water table elevations are recorded every 30 min with an accuracy of ± 2 mm. A typical diurnal (24-hr) response can be seen in the depth to water table (Figure 11). The water table data are shown for about 1 week before and after the 15 June 2006 wildfire for two wells at the Albuquerque South Valley site. The north well was not burned while the center well was burned but the pressure transducer and data logger continued to function. The diurnal pattern in water table depth with minimal levels in the late afternoon and maximal levels in the early morning may be responsive to riparian ET at the site. Continuation of the diel pattern in the burned well is possible due to the extensive root systems that cottonwood trees develop at depths cool enough to survive. An investigation is being made exploring the relationship between tower-based estimates of ET and the diurnal pattern of groundwater elevations. Initial documentation includes applying diurnal fluctuations of shallow alluvial groundwater to estimate plant uptake of groundwater and water salvage through non-native vegetation removal. These data allow a rigorous analysis of the possibility that diurnal fluctuations in groundwater elevations can be used to estimate riparian zone ET rates. The ability to compare estimated ET rates calculated from daily fluctuations in groundwater elevations with independently-derived tower-based ET measurements is a distinct aspect of the research that has not been reported in the literature to date.

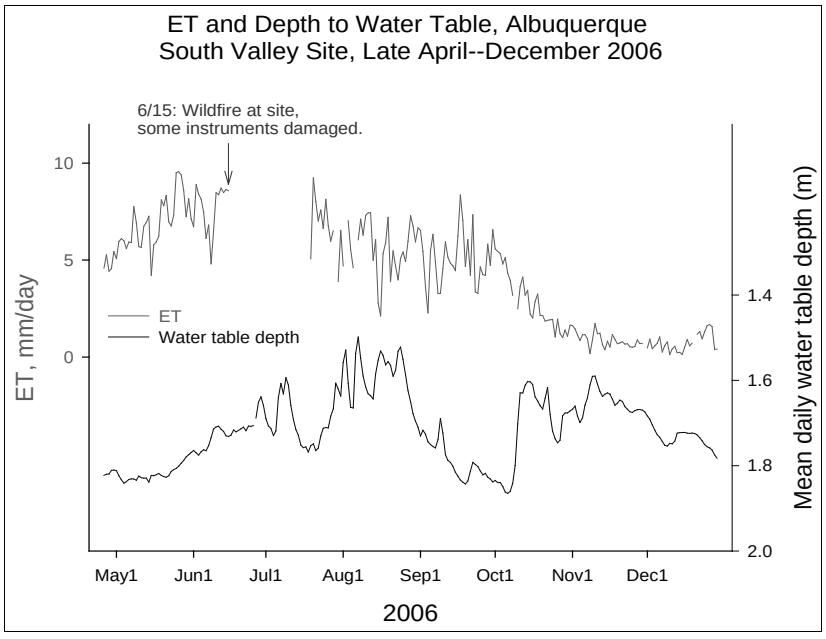

Figure 9. Depth to water table at Albuquerque South Valley ET site. Daily ET rates are graphed along with depth to water table for comparison. Some of water table sensors continued to work during and after fire so continuous record is available.

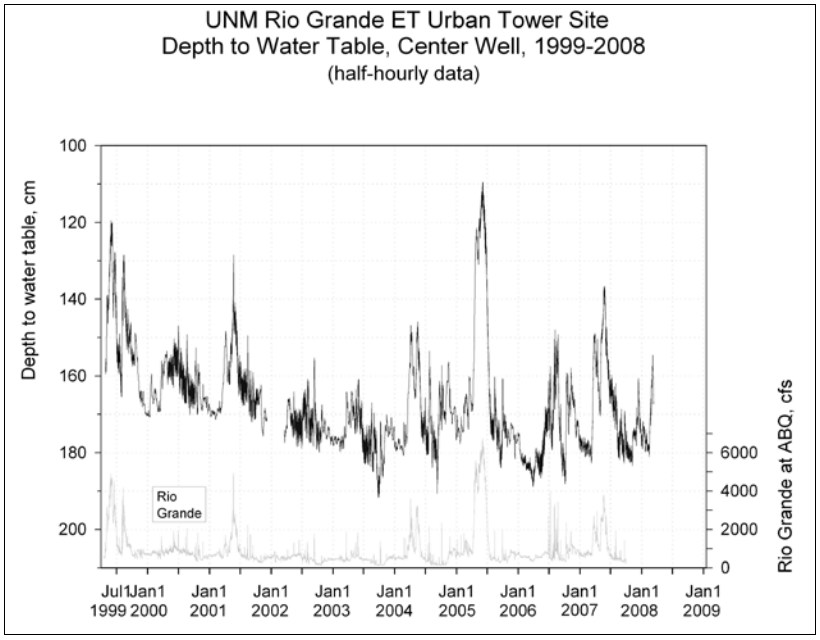

Figure 10. Long-term record of water table depth at Albuquerque South Valley site beginning in spring 1999. Discharge (Q) of Rio Grande at Central Bridge USGS gauging station is shown for comparison.

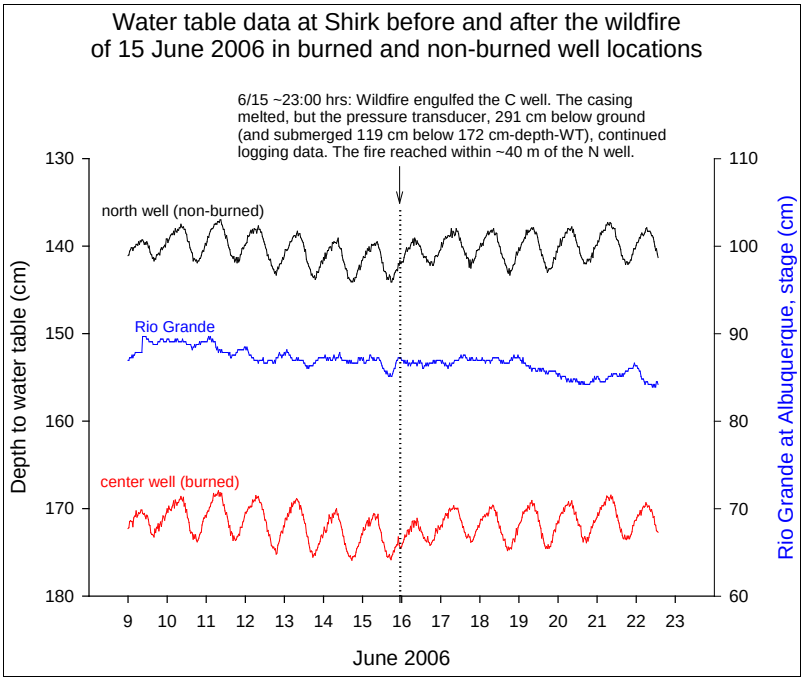

Figure 11. Daily water table data for two wells at Albuquerque South Valley site immediately before and after fire. The north well was not burned, center well was burned, but data logger and pressure transducer continued to function. The stage of Rio Grande at USGS Central Bridge gaging station is shown for comparison.

4 Remote Sensing

Overview

Scaling up the estimates of ET to an estimate of water use throughout the Urban Flood Demonstration Project area of interest requires remote sensing and Geographical Information Systems (GIS). In addition, multispectral remote sensing provides a tool to classify the riparian vegetation along the Rio Grande and to look for changes in vegetation or vegetative cover through time. Multispectral images from 2006 are compared to images from 2002 along the reach. Large changes in vegetation density due to fire, human construction activity, and understory removal between the two time periods are noted.

Methodology

Characterizing the landscape and classifying riparian canopy vegetation involves a series of procedures detailed in the flow diagram in Figure 12. First, cloud free images covering the area of interest are acquired and then processed. Files, generated from the processed images, provide the input to the Decision Tree Classifier (DTC). The input files consist of a mask that defines the active floodplain and rules based on the spectral response of landscape classes and subclasses. The classifier starts with a preliminary design. The design evolves after several iterations, where the results of each of the iterations are checked with the calibration points. After returning a successful run, (i.e., the returned classification matches the vegetation in the field at calibration points) further verification occurs in the field at river crossings and other readily accessible areas. As a final test, a Global Positioning System (GPS) capable field laptop is carried through several areas along the corridor with a final classification map on display. Once a DTC design produces a realistic representation of canopy vegetation, classification maps for the Albuquerque reach of the Middle Rio Grande of New Mexico are made for dates of interest when a cloud-free mosaic image is available.

DTCs perform multistage classifications based on “yes” or “no” answers to expressions or rules (Safavian and Landgrebe 1991). The rules and expressions are derived from a series of logical steps aimed at segregating classes. Each rule (parent node) splits the data into two groups (child

nodes) where the child nodes are purer than the parent node (Simard et al. 2002). The decision tree rules are based either on a physical location or on expressions derived from the spectral response of objects in the landscape. The first rule in the decision tree separates the area inside the levee roads from the historic floodplain. The area inside the levee roads represents the active floodplain. Using a heads-up display, a series of polygons are created over a panchromatic image. Road crossings over the river provide ideal edges to stop and start individual polygons. The final polygons are converted from a vector into a mask. In the decision tree, a mask of the active floodplain targets the specific rules to the masked area.

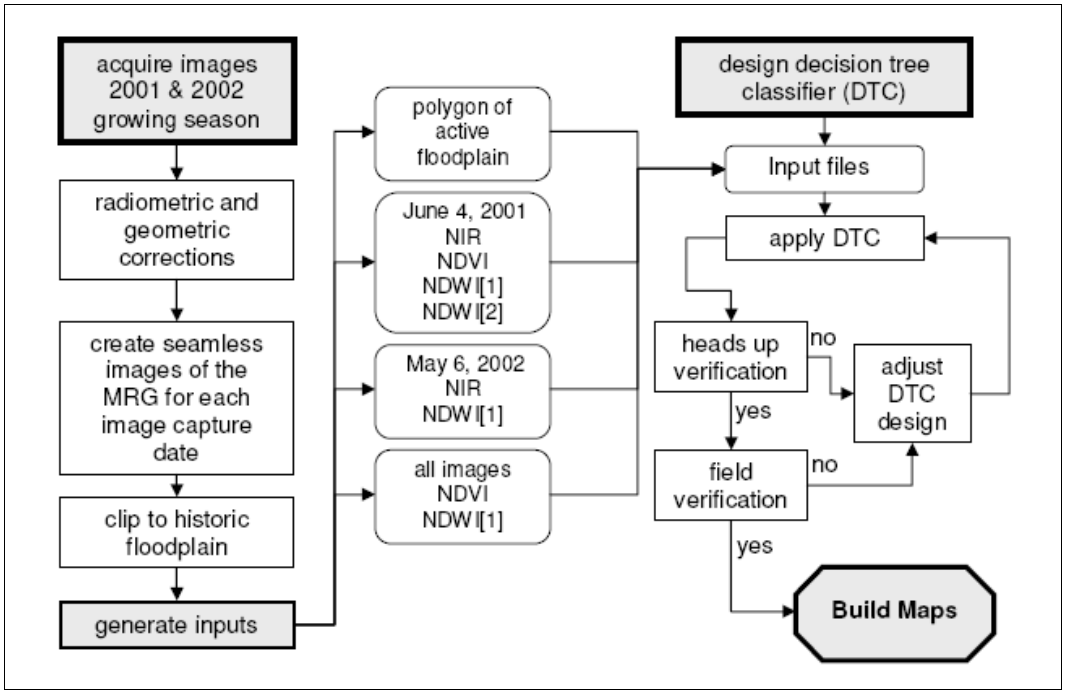

Figure 12. Schematic of procedures used to generate vegetation classification for bosque of Middle Rio Grande of New Mexico. Procedure is from McDonnell (2006).

The remaining expressions are based on the spectral response of landscape classes. Expressions based on red, near-infrared (NIR, Landsat 7 band 4, 760-900 nanometer), mid-infrared (MIR, Landsat 7 band 5, 1,550-1,750 nanometer), Normalized Difference Vegetation Index (NDVI), Normalized Difference Wetness Index number 1 (NDWI [1]), and Normalized Difference Wetness Index number 2 (NDWI [2]) are evaluated with each landscape class and canopy sub-class in order to develop the most efficient set of rules. In the end, expressions based on NIR, NDVI, NDWI [1], and NDWI [2] produce an efficient decision tree capable of separating out the broad landscape categories and then isolating the

canopy subclasses. The DTC, applied to each set of mosaic images, generates classification maps to compare the 2002 and 2006 images throughout the growing season. A detailed description of the methods used to produce the vegetation classification for the Rio Grande bosque in central New Mexico is found in McDonnell (2006).

Results

Figure 13 shows the Albuquerque reach of the Rio Grande riparian corridor with the City of Albuquerque overlain on the river and bosque. The riparian vegetation classification from 2002 multispectral remote sensing imagery is included (McDonnell 2006). The Albuquerque reach is subdivided into five subsections for more detailed characterization of the bosque. Locations of fires were obtained from shapefiles provided by the U.S. Army Engineer District, Albuquerque.

Figure 14 shows the northernmost section (section 1) of the river and riparian zone in the Albuquerque reach. The vegetation classification scheme is applied to a multispectral image from 2002 and 2006. No large fires occurred in this segment of the bosque during this period of time. Vegetation classes remained largely the same in this reach. The inset photograph on the 2006 image shows an area with increased amounts of surface water in 2006 from the strong summer monsoon of 2006 compared to 2002. The site is associated with the north Albuquerque drain.

Figure 15 compares the vegetation cover in 2002 and 2006 along the Albuquerque riverine corridor from just north of Paseo del Norte to just north of the Interstate 40 Bridge (section 2). This segment of the river and bosque was the site of the 2003 Montaño fire. The fire boundaries are shown on the 2006 image. Section 3 extends from just north of the I-40 Bridge to just north of Rio Bravo Boulevard (Figure 16). Key features that have changed in this reach between 2002 and 2006 are the Atrisco fire of 2003, the Conservancy fire of 2004, and the construction at Tingley Beach. The construction of wetlands in the bosque at the Tingley Beach area are shown in the insert photograph along with another area of change from understory clearing in the middle of the reach.

Section 4 of the Albuquerque reach extends from just north of the Rio Bravo Bridge to about 2.5 km north of the I-25 Bridge (Figure 17). Major changes to this reach in the period from 2002 to 2006 include the 2004 fire (the Brown fire) and the maintenance of the South Diversion Channel, including

vegetation removal shown in the photographs. Section 5 extends from about 2.5 km north of the I-25 Bridge to about 4.5 km south of the bridge (Figure 18). This section of the riverine corridor includes the ET tower and groundwater wells in the Albuquerque South Valley. The Malpais Fire of 15 June 2006 that extended to the access road to the ET tower is shown on the 2006 image with the fire in the bosque on both sides of the river with the majority of the fire immediately north of the I-25 Bridge.

Figure 19 compares NDVI from a 29 May 2006 SPOT satellite image with NDVI from an 24 August 2006 SPOT image. Large changes in NDVI are clearly visible in the Albuquerque South Valley due to the bosque wildfire of 15 June 2006.

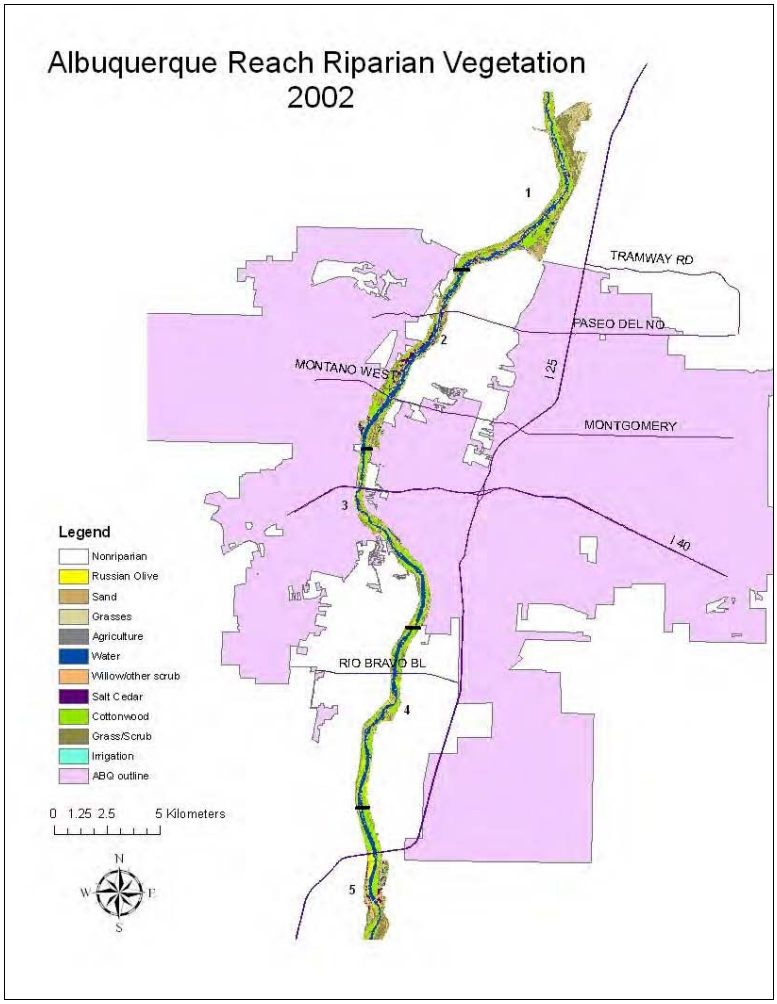

Figure 13. Study reaches for Urban Flood Demonstration Project and City of Albuquerque. Five reaches are delineated along this section of river corridor. Vegetation classification scheme from 2002 is applied to reach using multispectral remote sensing imagery.

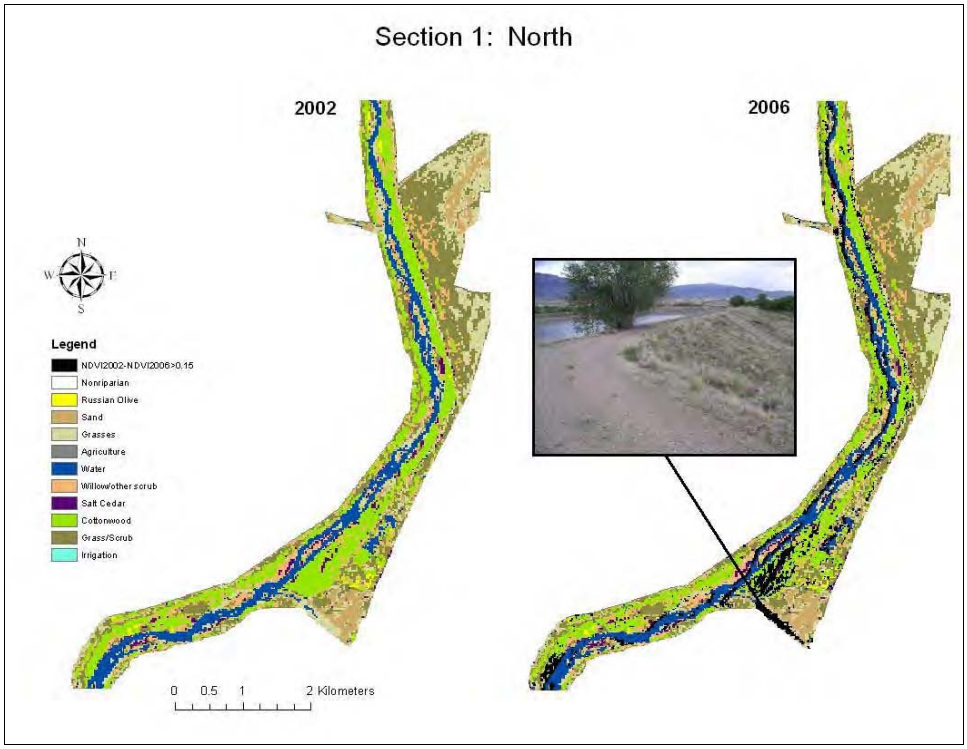

Figure 14. Section 1 of Albuquerque reach of Rio Grande corridor. Photograph shows additional water in North Diversion Channel in 2006 compared to 2002.

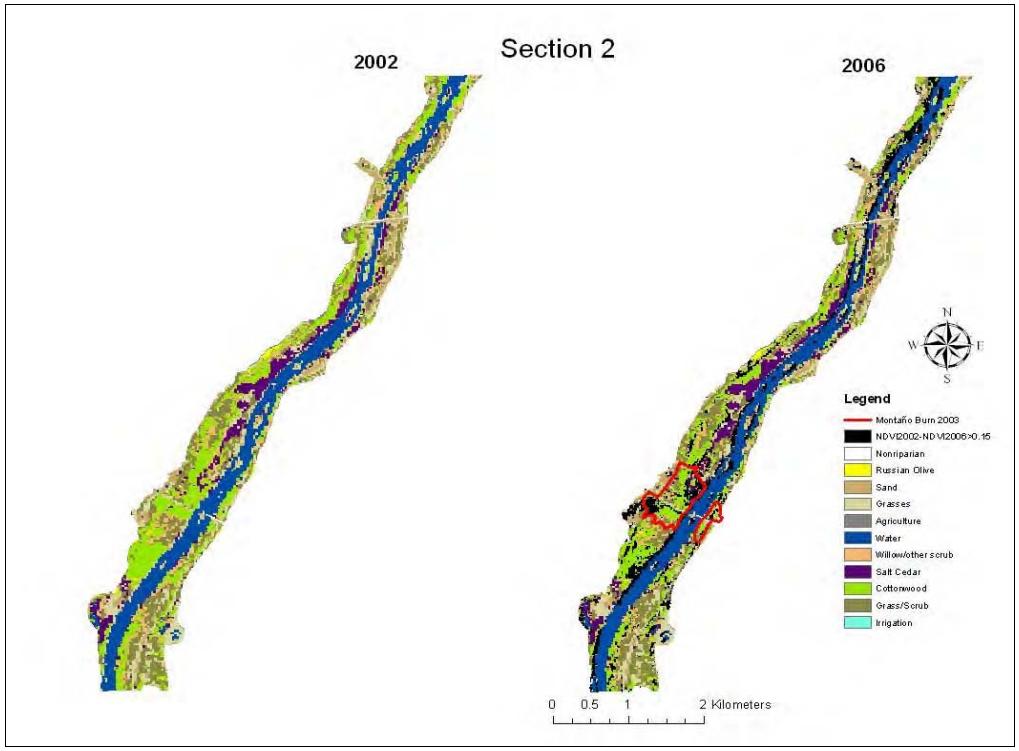

Figure 15. Section 2 of Albuquerque reach of Rio Grande corridor. Montaño fire site is shown on 2006 image.

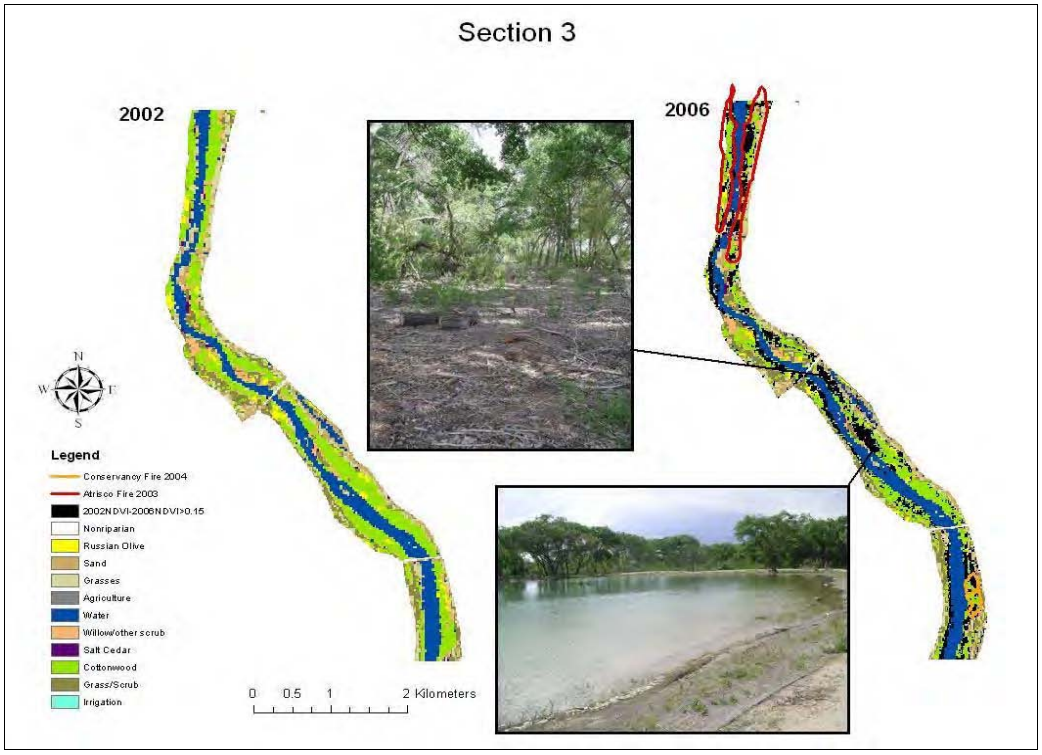

Figure 16. Section 3 of Albuquerque reach of Rio Grande corridor. New construction at Tingley Beach and understory removal of vegetation are shown in photographs in areas where vegetation characteristics had changed between 2002 and 2006. Atrisco fire and Conservancy fire also are shown in 2006 image.

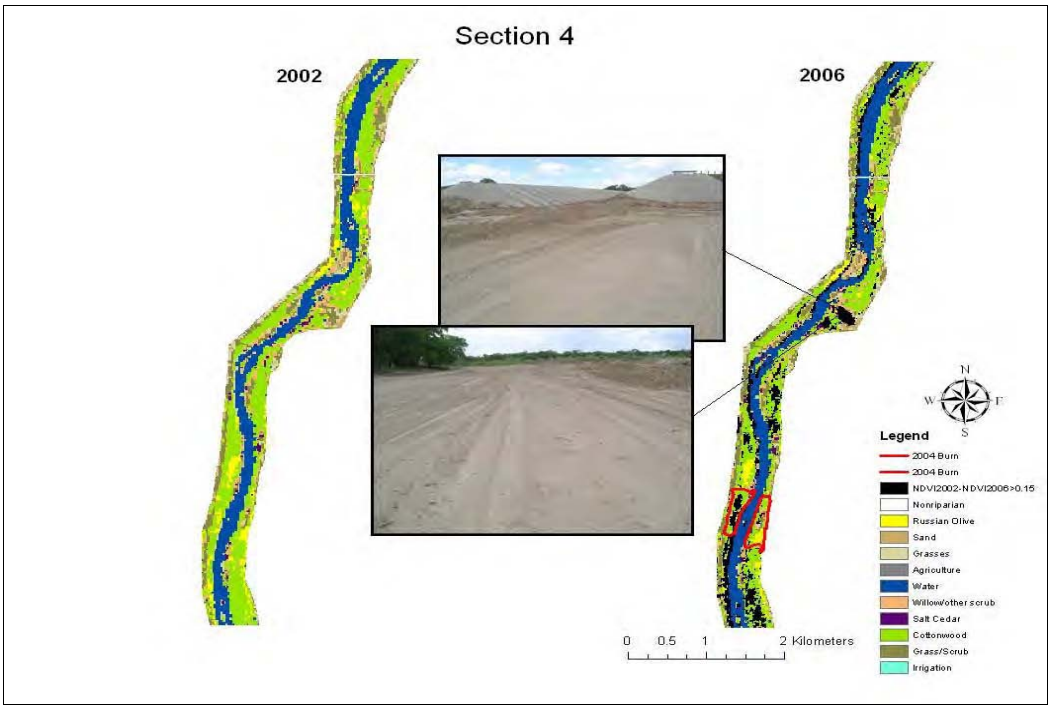

Figure 17. Section 4 of Albuquerque reach of Rio Grande corridor. The 2004 fires (Brown Fire) are included on 2006 image. An area of major vegetative change where maintenance of South Diversion Channel occurred is shown in photographs.

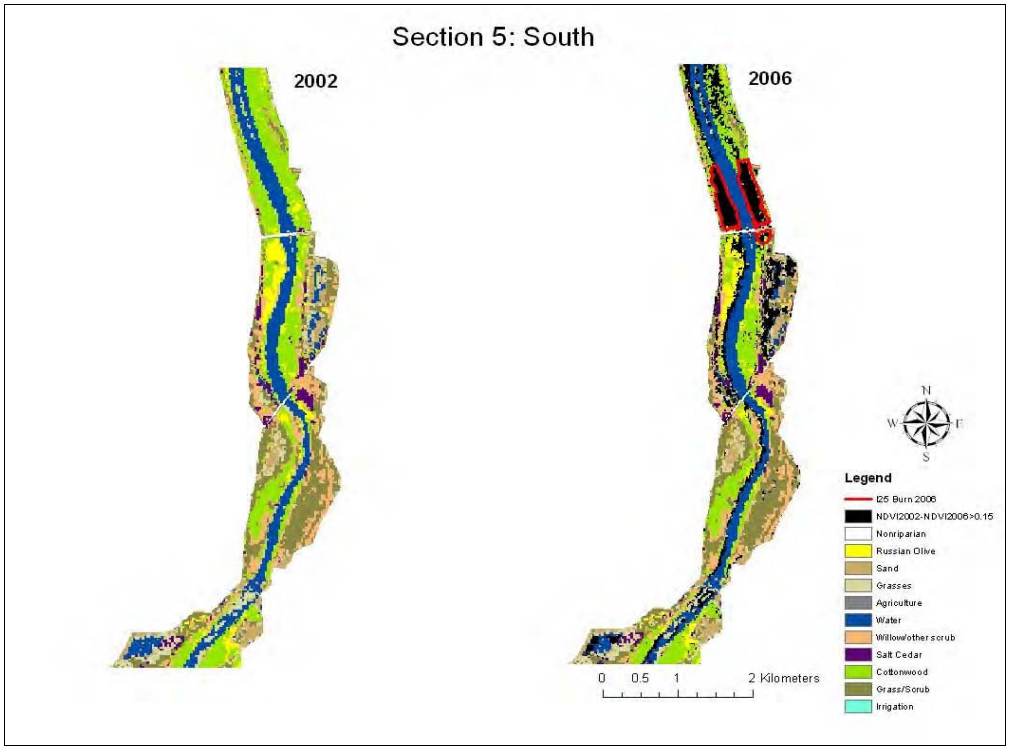

Figure 18. Southernmost section (section 5) of Albuquerque reach with vegetation classified for multispectral imagery obtained in 2002 and 2006. Malpais fire (15 June 2006) is delineated in upper third in 2006 image.

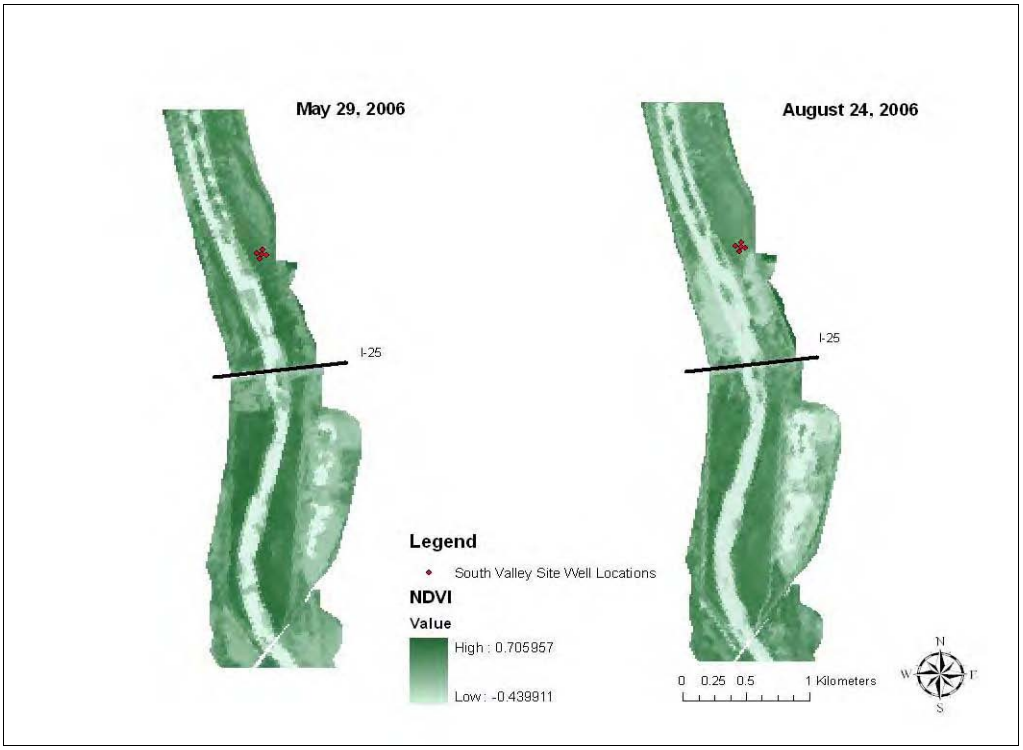

Figure 19. NDVI values are compared for SPOT imagery from 29 May 2006 and 24 August 2006. Fire areas with reduced NDVI from Malpais fire are clearly seen on both sides of river just to north of I-25 Bridge on 24 August 2006 image.

5 Water Table Flow Fields

Overview

The Alameda Diversion Dam has been constructed in the Albuquerque Reach. Identifying the effect of changing discharges on water table elevations downstream of the diversion structure is of great concern. The objective of this study is to calculate water table gradient changes during intervals of increasing river discharge.

Methodology

Figure 20 shows the location of the wells at the Alameda site and the points at which river stage was estimated. The points were chosen to be the intersections of the river and lines drawn between the outermost wells in Sites 2 and 3 and Sites 4 and 5, respectively. The river slope gradient is assumed to be 0.001 ft elevation change/ft river length, and the decrease in elevation was estimated as this slope multiplied by the distance of the river intersection points from the gage at Alameda Bridge. River data were downloaded from the USGS National Water Information System (USGS gage 08329918 *http://waterdata.usgs.gov/nwis*). Water table slope was recorded from points noted in Figure 20 as West Slope and East Slope. These points are equidistant from the two center wells on each side of the river.

To examine how the water table gradient changes as river stage changes, two intervals of increasing discharge were selected. One interval was in May when discharge would be driven by snowmelt, and one was in August when the change in stage would be due to monsoonal precipitation (Figure 21). Events circled in green were used for the analysis.

At 1-hr intervals during each event, a Triangulated Irregular Network (TIN) was constructed using the water table elevation data for all wells, estimated river elevation, and monthly measurements of riverside drain water level elevations that were collected by the Bosque Ecosystem Monitoring Program (BEMP (http://www.bosqueschool.org/bemp.htm)). An example of such a TIN is shown in Figure 22.

Results

During the 7-hr interval monitored on 2 May 2007 river stage increased 0.13 m, the aspect of the gradient monitored on the west side of the river changed from 291.851 to 294.937 deg and water table elevation increased 0.064 m. On the east side of the river, the aspect of the gradient changed from 123.189 to 123.021 deg and elevation increased 0.002 m.

During the 7-hr interval monitored on 31 July/1 August, river stage increased 0.63 m and then fell again. The aspect of the gradient monitored on the west side of the river changed from 291.85 to 293.69 deg and water table elevation increased 0.212 m. On the east side of the river, the aspect of the gradient changed from 123.35 to 123.18 deg and the elevation increased 0.087 m. Figures 23 and 24 show how the slope of the gradient changed with respect to the river stage on 2-3 May and 31 July/1 August 2007 on both sides of the river.

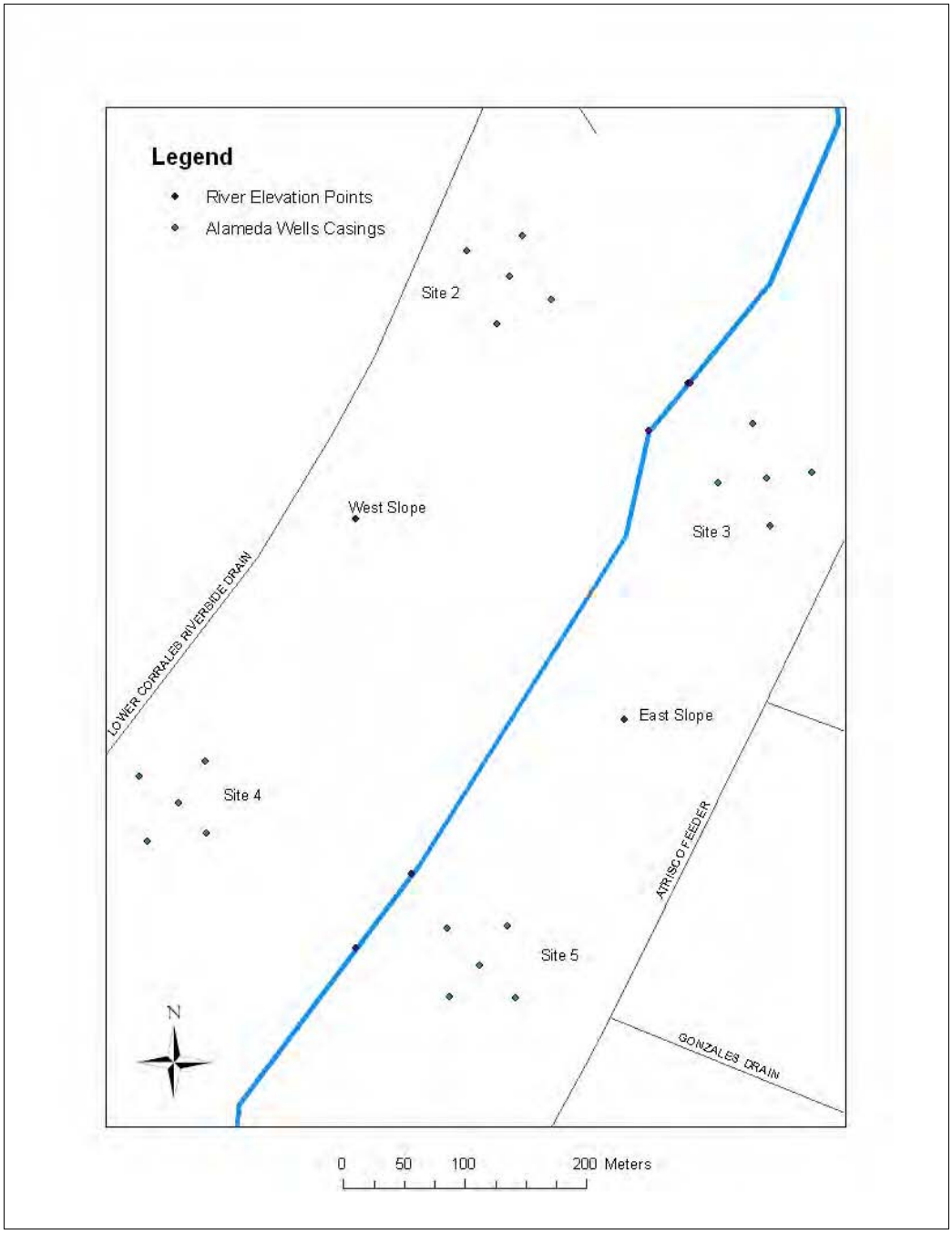

Figure 20. Location of Alameda Site wells, points at which elevation of river was estimated, and points where water table slope were estimated from TINs.

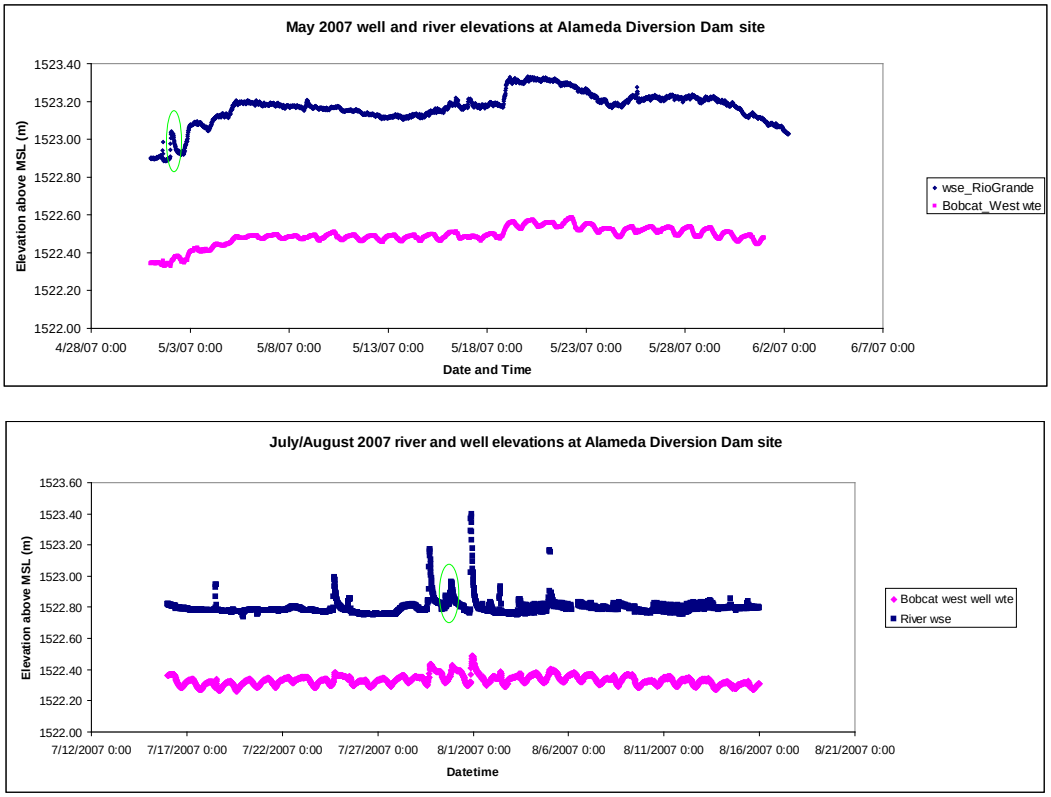

Figure 21. Elevation of water table and river during May 2007 and mid-July to mid-August 2007. Green circles designate the events used to assess water table gradient change.

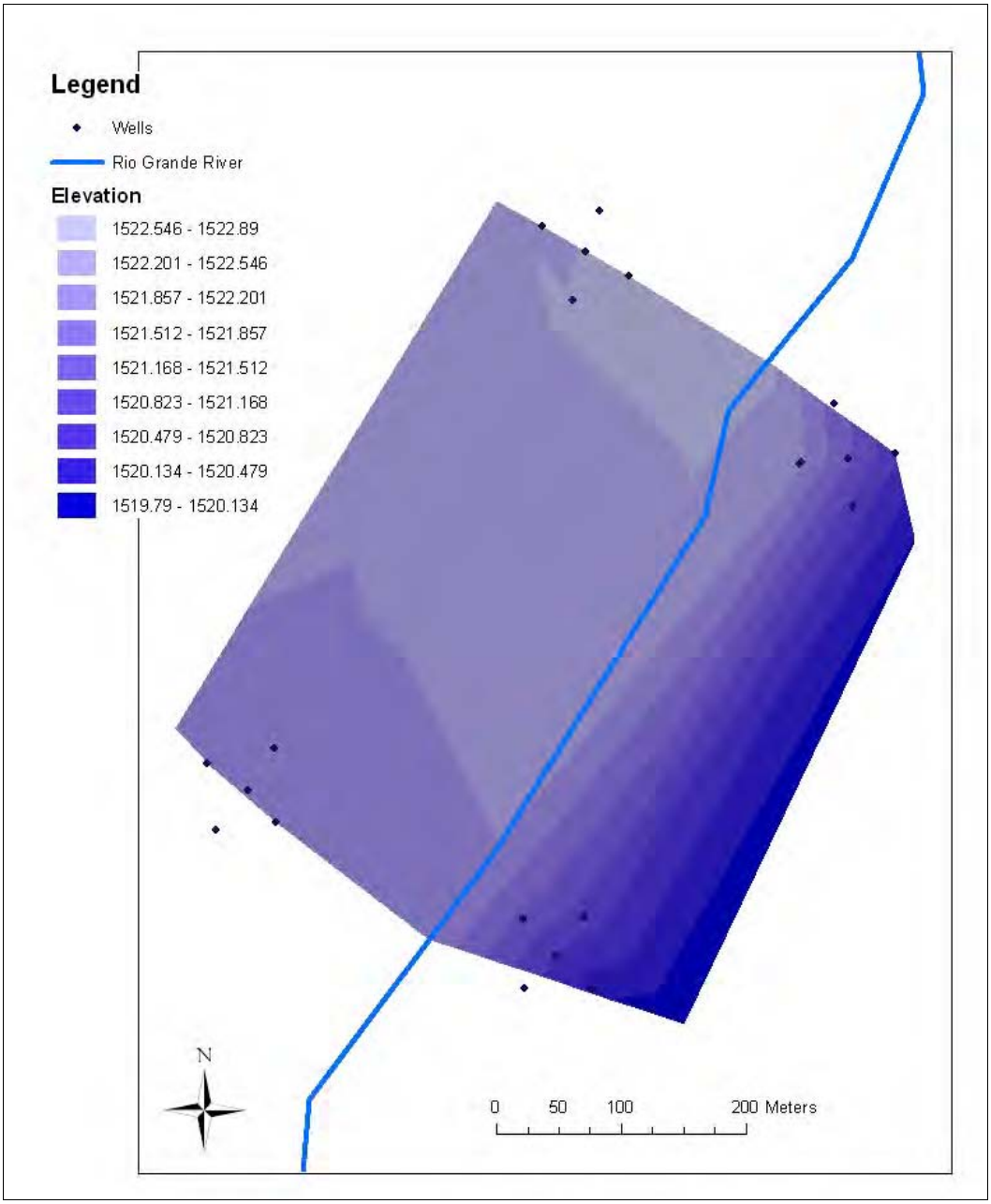

Figure 22. TIN of Alameda Diversion Dam site from Lower Corrales Drain on west to Atrisco Feeder Drain on east at 7 p.m. on 31 July 2007. Note that data are not available for all five wells at each site (all units are in meters).

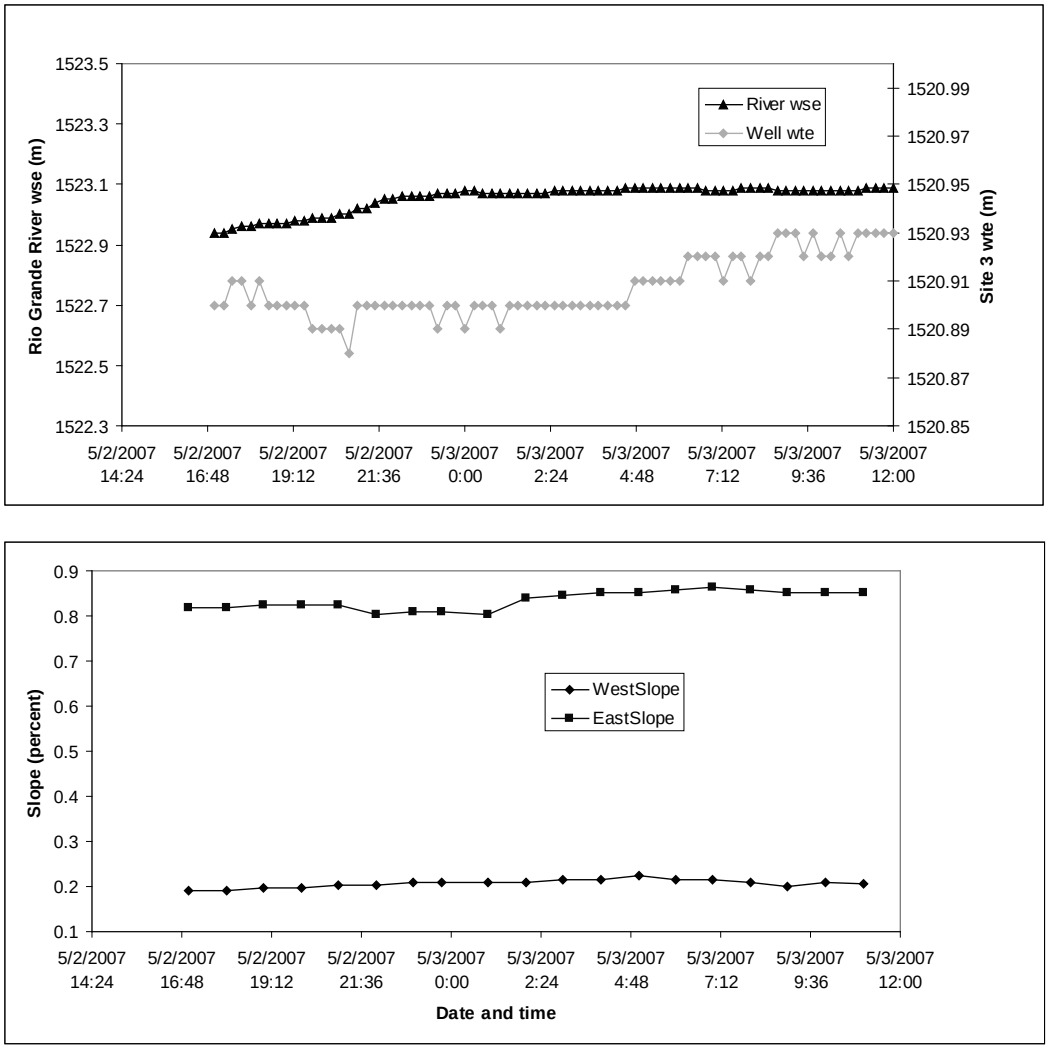

Figure 23. Elevation of river and groundwater on 2-3 May (upper figure). Change in slope of water table during this interval is also displayed (lower figure).

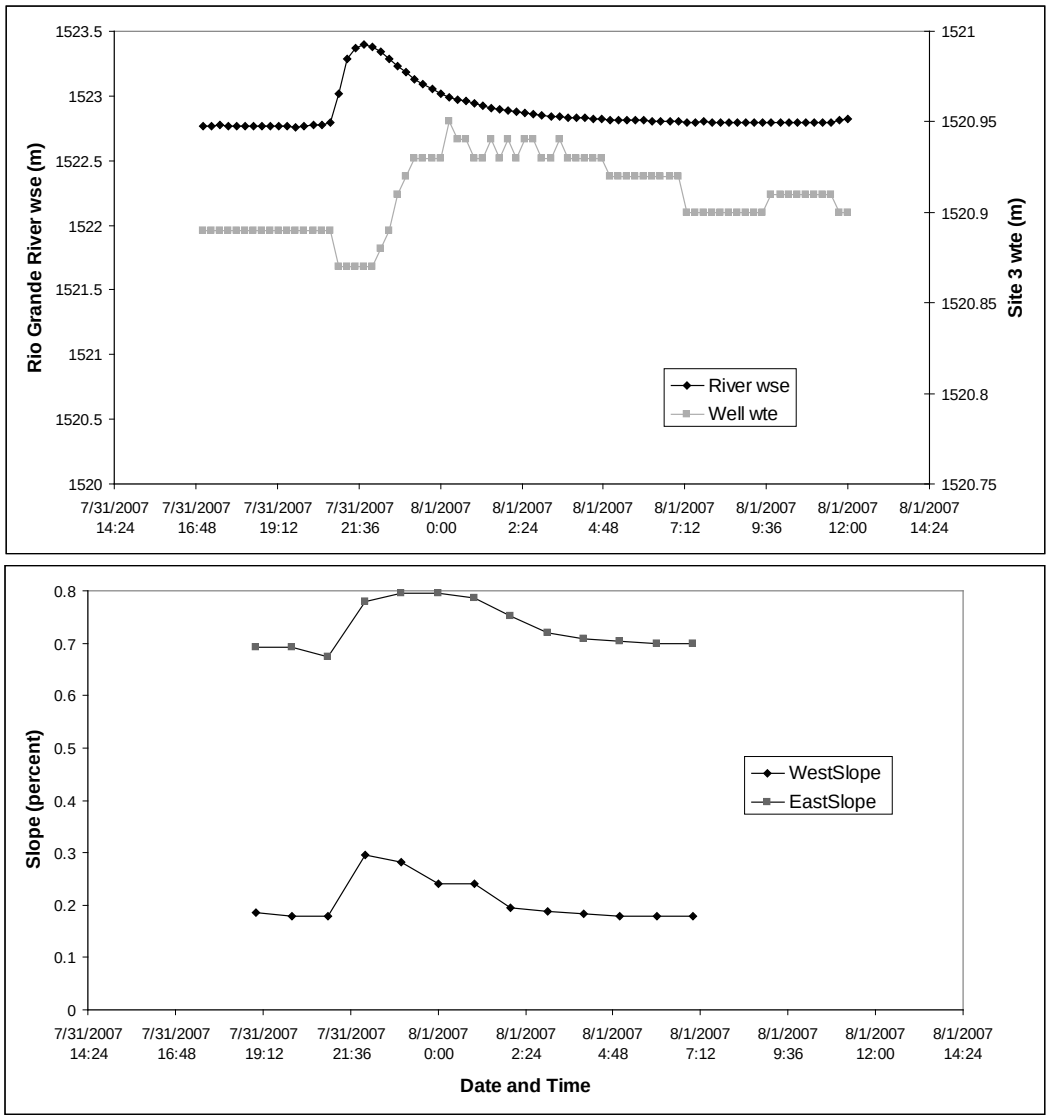

Figure 24. Elevation of river and groundwater on 31 July/1 August (upper figure). The change in slope of water table during this interval is also displayed (lower figure).

6 Summary and Conclusions

Funding through the UFDP and SWDP has allowed the continued measurement of ET rates using state-of-the-art 3-D eddy covariance techniques at a non-flooding cottonwood-dominated riparian zone in a reach of Rio Grande where overbank flooding no longer occurs. The growing season of 2006 included a human-caused bosque fire on 15 June 2006 (the Malpais fire) that burned up to the access road to the tower site. The fire offers the opportunity to assess the effects of wildfire in the bosque on ET rates and to follow the recovery from the fire as new riparian vegetation germinates and some of the burned vegetation resprouts. The instruments damaged were replaced about 1 month after the fire, and ET rates were gathered throughout the rest of the 2006 growing season (late July through November).

Water table measurements were made throughout 2006 and are continuing in 2007 and 2008 at four of the wells at the site with the ET tower. The wells are highly responsive to discharge and stage in the Rio Grande. Lower water tables occurred during the abnormally dry winter and spring of 2006. The exceptionally strong summer monsoons of 2006 caused floods in the Rio Grande that raised the water table multiple times at the ET site. A clear diurnal pattern in the water table may provide an independent method for estimating ET rates. Ongoing research is (1) evaluating the accuracy of using diurnal fluctuations to estimate ET rates by comparing the magnitude of daily fluctuations to ET rates determined by the 3-D eddy covariance methodology deployed on the tower, and (2) identifying groundwater flow fields that develop as a response to changes in river and drain discharge.

Remote sensing analyses using multispectral SPOT imagery allowed comparison of the vegetation within the bosque in the Albuquerque reach in 2006 to an earlier 2006 assessment from LANDSAT imagery. Major changes in the vegetation within the reach are linked to fires, construction activity, and understory thinning operations. Vegetation classification can ultimately be coupled with estimates of vegetation density and the tower-based measurements of ET rates in various vegetation types to generate spatially explicit estimates of ET rates along the riverine corridor of the Rio Grande.

References

Brunet, Y., B. Itier, J. McAneney, and J. P. Lagouarde. 1994. Downwind evolution of scalar fluxes and surface resistance under conditions of local advection. Part II: Measurements over barley. *Agricultural and Forest Meteorology* 71(3):227-245.

Cleverly, J. R., C. N. Dahm, J. R. Thibault, D. J. Gilroy, and J. E. A. Coonrod. 2002. Seasonal estimates of actual evapo-transpiration from *Tamarix ramosissima* stands using three-dimensional eddy covariance. *Journal of Arid Environments* 52(2):181-197.

Cleverly, J. R., C. N. Dahm, J. R. Thibault, D. E. McDonnell, and J. E. A. Coonrod. 2006. Riparian ecohydrology: Regulation of water flux from the ground to the atmosphere in the Middle Rio Grande, New Mexico. *Hydrological Processes* 20(15):3,207-3,225.

Cooper, D, W. Eichinger, J. Archuleta, L. Hipps, J. Kao, M. Leclerc, C. Neale, and J. Prueger. 2003. Spatial source-area analysis of three-dimensional moisture fields from LIDAR, eddy covariance, and a footprint model. *Agricultural and Forest Meteorology* 114(3):213-234.

Cooper, D. I., W. E. Eichinger, J. Kao, L. Hipps, J. Reisner, S. Smith, S. M. Schaeffer, and D. G. Williams. 2000. Spatial and temporal properties of water vapor and latent energy flux over a riparian canopy. *Agricultural and Forest Meteorology* 105(1):161-183.

Dahm, C. N., J. R. Cleverly, J. E. A. Coonrod, J. R. Thibault, D. E. McDonnell, and D. F. Gilroy. 2002. Evapotranspiration at the land/water interface in a semi-arid drainage basin. *Freshwater Biology* 47(4):831-843.

Drexler, J. Z., R. L. Snyder, D. Spano, and Paw U, K. T. 2004. A review of models and micrometeorological methods used to estimate wetland evapotranspiration, *Hydrological Processes* 18(11):2,071-2,069.

Goodrich, D. C., R. Scott, J. Qi, B. Goff, C. L. Unkrich, M. S. Moran, D. Williams, S. Schaeffer, K. Snyder, R. MacNish, T. Maddock, D. Pool, A. Chehbouni, D. I. Cooper, W. E. Eichinger, W. J. Shuttleworth, Y. Kerr, R. Marsett, and W. Ni. 2000. Seasonal estimates of riparian evapotranspiration using remote and in situ measurements. *Agricultural and Forest Meteorology* 105(1):281-309.

Kao, C. Y. J., Y. H. Hang, D. I. Cooper, W. E. Eichinger, W. S. Smith, and J. M. Reisner. 2000. High-resolution modeling of LIDAR data mechanisms governing surface water vapor variability during SALSA. *Agricultural and Forest Meteorology* 105(1):185-194.

Massman, W. 2000. A simple method for estimating frequency response corrections for eddy covariance systems. *Agricultural and Forest Meteorology* 104(3):185-198.

Massman, W. 2001. Reply to comment by Rannik on "A simple method for estimating frequency response corrections for eddy covariance systems." *Agricultural and Forest Meteorology* 107(3):247-251.

McAneney, K. J., Y. Brunet, and B. Itier. 1994. Downwind evolution of transpiration by two irrigated crops under conditions of local advection. *Journal of Hydrology* 161(1-4): 375-388.

McDonnell, D. E. 2006. Scaling riparian evapotranspiration to canopies along the Middle Rio Grande corridor in central New Mexico. Ph.D. dissertation, 189 p. Albuquerque, NM: University of New Mexico.

Nakamura, R., and L. Mahrt. 2001. Similarity theory for local and spatially averaged momentum fluxes. *Agricultural and Forest Meteorology* 108(4):265-279.

Rannik U., M. Aubinet, O. Kurbanmuradov, K. Sabelfeld, T. Markkanen, and T. Vesala. 2000. Footprint analysis for measurements over a heterogeneous forest. *Boundary-Layer Meteorology* 97(1):137-166.

Safavian, S. R., and D. Landgrebe. 1991. A survey of Decision Tree Classifier methodology. Institute of Electrical and Electronics Engineers *Transactions on Geoscience and Remote Sensing* 21(3):660-674.

Scott, R. L., W. J. Shuttleworth, D. C. Goodrich, and T. Maddock. 2000. The water use of two dominant vegetation communities in a semiarid riparian ecosystem. *Agricultural and Forest Meteorology* 105(1):241-256.

Shafroth, P. B., J. R. Cleverly, T. L. Dudley, J. P. Taylor, C. Van Riper, E. P. Weeks, and J. N. Stuart. 2005. Control of Tamarix in the western United States: Implications for water salvage, wildlife use, and riparian restoration. *Environmental Management* 35(3):231-246.

Simard, M, G. D. Grandi, S. Saatchi, and P. Mayaux. 2002. Mapping tropical coastal vegetation using JERS-1 and ERS-1 radar data with a decision tree classifier. International Journal of Remote Sensing 23(7):1461-1474.

Simpson, I. J., G. W. Thurtell, H. H. Neumann, G. Den Hartog, and G. C. Edwards. 1998. The validity of similarity theory in the roughness sublayer above forests. *Boundary-Layer Meteorology* 87(1):69-99.

Stull, R. B. 1988. *An Introduction to Boundary Layer Meteorology*. Boston, MA: Kluwer Academic Publishers.

Twine, T. E., W. P. Kustas, J. M. Norman, D. R. Cook, P. R. Houser, T. P. Meyers, J. H. Prueger, P. J. Starks, and M. L. Wesely. 2000. Correcting eddy-covariance flux underestimates over a grassland. *Agricultural and Forest Meteorology* 103(3):279-300.

Webb, E, G. Pearman, and R. Leuning. 1980. Correction of flux measurements for density effects due to heat and water-vapor transfer. *Quarterly Journal of the Royal Meteorological Society* 106(447):85-100.

Wesely, M. L. 1970. Eddy Correlation Measurements in the Atmospheric Surface Layer over Agricultural Crops. Ph.D. dissertation, 102 p. Madison, WI: University of Wisconsin.

REPORT DOCUMENTATION PAGE

Form Approved
OMB No. 0704-0188

1. REPORT DATE *(DD-MM-YYYY)*	2. REPORT TYPE	3. DATES COVERED *(From - To)*
September 2010	Final Report	

4. TITLE AND SUBTITLE

Evapotranspiration, Water Table Fluctuations, and Riparian Restoration: Report Documentary 2007-2008 Work

5a. CONTRACT NUMBER

5b. GRANT NUMBER

5c. PROGRAM ELEMENT NUMBER

6. AUTHOR(S)

James R. Cleverly, Kristin Vanderbilt, Cliff Dahm,
James R. Thibault, and Maceo Carrillo Martinet

5d. PROJECT NUMBER

5e. TASK NUMBER

5f. WORK UNIT NUMBER

7. PERFORMING ORGANIZATION NAME(S) AND ADDRESS(ES)

University of New Mexico
MSC01 1070 Civil Engineering
Albuquerque, NM 87120

8. PERFORMING ORGANIZATION REPORT NUMBER

ERDC/CHL CR-10-4

9. SPONSORING / MONITORING AGENCY NAME(S) AND ADDRESS(ES)

U.S. Army Corps of Engineers
Coastal and Hydraulics Laboratory
3909 Halls Ferry Road
Vicksburg, MS 39180-6199

10. SPONSOR/MONITOR'S ACRONYM(S)

11. SPONSOR/MONITOR'S REPORT NUMBER(S)

12. DISTRIBUTION / AVAILABILITY STATEMENT

Approved for public release; distribution is unlimited.

13. SUPPLEMENTARY NOTES

14. ABSTRACT

Water use by riverside phreatophyte ecosystems, also referred to as evapotranspiration or just ET, makes up a significant proportion of a river basin's water budget depletions. As phreatophytes, riparian plants access groundwater for their water supply. The objective of this study is to characterize ET depletions from various representative riparian land cover types and to describe the groundwater-vegetation interactions that relate ET to local hydrology. Measurements of ET and groundwater are made at various locations within the city of Albuquerque, NM, and along the Middle Rio Grande. ET is measured from eddy covariance flux towers and groundwater levels are continuously monitored using commercially available submersible pressure transducers. Results show that modest water salvage can be claimed from riparian restoration projects that are properly implemented while additional water losses are possible when necessary follow-up is not undertaken. Bare soil is shown to lose less water to evaporation than previously expected, and urban hydrology (e.g., waste water return) maintains high ET rates in whichever species grow in the outfall. Remote sensing of riparian vegetation clearly shows the effects of fires in the urban reach, the initial decline in vegetation density, leaf area index, and ET. This research illustrates the importance of identifying the hydrologic and vegetative factors controlling ET in a large, urban river system.

15. SUBJECT TERMS

Ecosystems
Evapotranspiration
Groundwater
Phreatophytes
Riparian restoration
River basin
Urban River system

16. SECURITY CLASSIFICATION OF:			17. LIMITATION OF ABSTRACT	18. NUMBER OF PAGES	19a. NAME OF RESPONSIBLE PERSON
a. REPORT	b. ABSTRACT	c. THIS PAGE			19b. TELEPHONE NUMBER *(include area code)*
UNCLASSIFIED	UNCLASSIFIED	UNCLASSIFIED		44	